UNIVERSITY OF TROMSØ UIT

FACULTY OF HEALTH SCIENCES
DEPARTMENT OF CLINICAL MEDICINE

MAGNETIC RESONANCE IMAGING OF PANCREATIC ISLETS TRANSPLANTATION

An experimental study in mice and baboons

Natalia V. Evgenov

A dissertation for the degree of
Philosophiae Doctor

August 2012

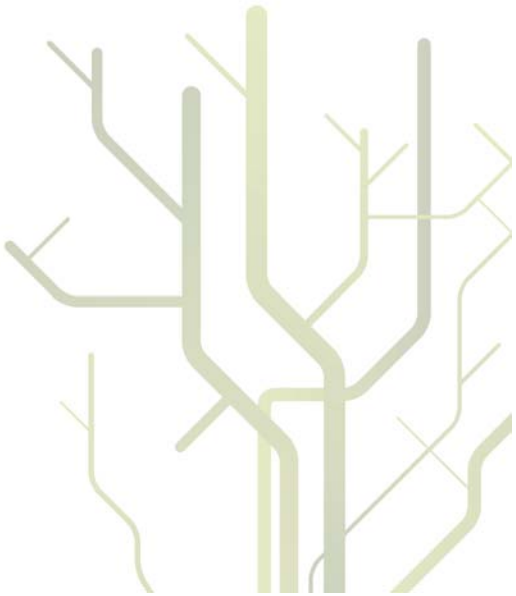

MAGNETIC RESONANCE IMAGING OF PANCREATIC ISLETS TRANSPLANTATION

An experimental study in mice and baboons

Natalia V. Evgenov, M.D.

A dissertation for the degree of Philosophiae Doctor

Athinoula A. Martinos Center for Biomedical Imaging
Department of Radiology
Massachusetts General Hospital
Harvard Medical School
Boston, Massachusetts, USA

Department of Clinical Medicine
Faculty of Health Sciences
University of Tromsø
Tromsø, Norway

2012

… to my family
for supporting me each step of the way

“It is better to light a candle than to curse the darkness.”

– *Chinese proverb*

Contents

1. Acknowledgements

During my several years of research training at the University of Tromsø and Harvard University, I have had the great privilege of working with many talented and compassionate individuals who have made important contributions to my development as a researcher. I would like to emphasize that the studies presented in this thesis are the result of a solid teamwork.

First of all, I wish to express my deepest gratitude to my scientific supervisor Dr. Anna Moore for encouraging me to undertake these studies, for providing excellent scientific guidance, and also for her enthusiasm, optimism, endless generosity, support and patience. Dr. Moore has been an excellent role model for me due to her truly inspiring and remarkable dedication and commitment to science.

It is also with great pleasure that I wish to thank my administrative supervisor Dr. John-Bjarne Hansen for his generous support and wise guidance during the formal parts of my research education and his advice and assistance in refining this thesis and the preparations for its defense.

I would like to express my gratitude to the Director of the Athinoula A. Martinos Center for Biomedical Imaging, Dr. Bruce Rosen. This dissertation would not have been possible without the efforts made by Dr. Rosen in promoting and supporting a stimulating rich academic and social environment in the department. I also am truly indebted and thankful to Dr. Susan Bonner-Weir from the Joslin Diabetes Center for sharing her expertise in diabetes and islets transplantation and offering wise advices.

I owe sincere and earnest thankfulness to my colleague Dr. Zdravka Medarova, who assisted, advised, supported and contributed to my research and writing over the years. I would like to thank John Pratt not only for his valuable contribution to the study but also for his friendship and support. I express my deep appreciation to Guangping (George) Dai for the exceptional technical support and knowledge of magnetic resonance imaging. My thanks also go out to Pamela Pantazopoulos for her excellent research assistance, kindness and patience. I would like to acknowledge John Moore and Jennifer Hollister-Lock for their exceptional technical support with animal surgeries.

I would particularly like to thank Dr. Jon Florholmen for introducing me to the world of medical research and for his kindness and generosity. I would also like to acknowledge support of Dr. Ruth Paulssen. In addition, I sincerely thank Ingrid Christiansen, Jorunn Eikrem, Åse Lund, Hege Appelbom, Birgit Svensson, and Åse Vårtun for their kindness and teaching me numerous laboratory skills.

I am very grateful to Dr. Elena Egorina and Dr. Mikhail Sovershaev for giving me a new appreciation for the meaning and importance of friendship. I also thank Dr. Marina Romantzova and Dr. Nina Gagarina whose friendship and wisdom have supported, enlightened, and entertained me over the many years.

None of this could have happened without the invaluable help, encouragement, support, great patience, and love of my husband. I am also very grateful to my sons for “building my character”. Most importantly, I wish to thank my parents and my extended family in Russia for their support, unconditional love and for teaching me the right values.

Finally, it is with sincere and heartfelt gratitude that I thank the Medical Faculty of the University of Tromsø for the opportunity to defend my thesis.

Natalia V. Evgenov, M.D.
June 2012

2. List of Papers

This thesis is based on the following papers, which are referred in the text by their Roman numerals:

I. Evgenov NV, Medarova Z, Dai G, Bonner-Weir S, Moore A. In vivo imaging of islet transplantation. *Nat Med* 2006; 12: 144-148.

II. Medarova Z, Evgenov NV, Dai G, Bonner-Weir S, Moore A. In vivo multimodal imaging of transplanted pancreatic islets. *Nat Protoc* 2006; 1: 429-435.

III. Evgenov NV, Medarova Z, Pratt J, Pantazopoulos P, Leyting S, Bonner-Weir S, Moore A. In vivo imaging of immune rejection in transplanted pancreatic islets. *Diabetes* 2006; 55: 2419-2428.

IV. Evgenov NV, Pratt J, Pantazopoulos P, Moore A. Effects of glucose toxicity and islet purity on in vivo magnetic resonance imaging of transplanted pancreatic islets. *Transplantation* 2008; 85: 1091-1098.

V. Medarova Z, Vallabhajosyula P, Tena A, Evgenov N, Pantazopoulos P, Tchipashvili V, Weir G, Sachs D, Moore A. In vivo imaging of autologous islet grafts in the liver and under the kidney capsule in non-human primates. *Transplantation* 2009; 87: 1659-1666.

3. Abbreviations

18F-FDG	18F-fluorodeoxyglucose
Balb/C	an albino laboratory-bred strain of the house mice
BLI	bioluminescence optical imaging
CD	cluster of differentiation
CITR	Collaborative Islet Transplant Registry
CT	Computerized tomography
ECM	extracellular matrix
FIONs	polyethylene glycol-phospholipid (PEG-phospholipid)-encapsulated magnetite nanocubes
GLP-1R	glucagon-like peptide 1 receptor
H	hydrogen
HbA1c	glycated hemoglobin
HSV1-sr39tk	herpes simplex virus 1 thymidine kinase
IBMIR	blood-mediated inflammatory reaction
ITR	Islet Transplant Registry
T1DM	type 1 diabetes mellitus
MHC	major histocompatibility complex
MN-NIRF	magnetic nanoparticles modified with the near-infrared fluorescent Cy5.5 dye
MRI	magnetic resonance imaging
NOD-SCID	Nonobese Diabetic–Severe Combined Immunodeficient Mice
nu/nu	Nude Mice
PET	Positron emission tomography
T	Tesla
T1	spin-lattice relaxation time
T2	spin-spin relaxation time
ROS	reactive oxygen species

4. General Introduction

Pancreatic islet transplantation can provide glycemic control and insulin independence for patients with type 1 diabetes. Pancreatic islets are highly vulnerable during the immediate post-transplantation period. Long-term monitoring of transplanted islets with a reliable and noninvasive imaging technology is an unmet clinical need. The main goal of the present studies was to develop a technique for *in vivo* visualization of human pancreatic islets transplanted in mouse and baboon models of Type 1 diabetes mellitus using a high-resolution magnetic resonance imaging (MRI).

4.1 Type 1 Diabetes Mellitus

Type 1 diabetes mellitus (T1DM) is one of the most common endocrine problems in childhood and adolescence, and remains a serious chronic disorder with increased morbidity and mortality and reduced quality of life [1]. According to the American Centers for Disease Control about 1.3 million people in the United States have T1DM. More than 13,000 young people are diagnosed with T1DM each year [2]. In Europe, the incidence of T1DM in children younger than 15 years increases by 3.9% annually. If a present trend continues, doubling of new cases of T1DM in European children younger than 5 years is predicted by 2020, and prevalent cases younger than 15 years will rise by 70% [3]. Medical management of patients with T1DM is associated with a six- to sevenfold higher direct costs than medical management of the age-matched non-diabetics [4].

Type 1 diabetes mellitus is chronic autoimmune disease in genetically predisposed individuals clinically characterized by hyperglycemia [5]. Regulation of blood glucose concentrations requires an adequate number of functioning pancreatic beta-cells able to respond to fluctuating glucose levels by secreting insulin. Pancreatic islets or the islets of Langerhans are vascularized clusters of cells within the pancreas that contain the insulin-producing beta-cells. They were named after Paul Langerhans who provided the first comprehensive description of their histology in his dissertation in 1869 [6]. There are five types of cells within an islet: α, β, δ, pp, and ε cells that secrete glucagon, insulin, somatostatin, pancreatic polypeptide, and ghrelin, respectively. In islets, there are 36.4-72.4% of insulin-positive cells, 12.4-48.2 % of glucagon-positive cells, 2.9-29.5% of somatostatin-positive cells, 0.5-4.2% of pancreatic polypeptide-positive cells [7]. In diabetic patients, a targeted inflammatory reaction against insulin secreting beta-cells in the islets of Langerhans results in a gradual loss of beta-cells [8, 9]. In order to maintain physiological levels of blood glucose, patients require lifelong insulin replacement therapy combined with tailored diet and physical exercise [10].

4.2 Current Management of Type 1 Diabetes

Insulin replacement therapy is based on multiple insulin injections and frequent assessment of glycemic control. Diabetic patients with poor glycemic control experience numerous life threatening, disease-associated microvascular (retinopathy, neuropathy, and nephropathy) and macrovascular (coronary and peripheral vessel disease) complications [10]. The goal of the

intensive insulin therapy is to keep the blood glucose level within the normal range. Long-term maintenance of euglycemia significantly delays the progression of chronic diabetic complications [11-13]. Nevertheless, intensive insulin therapy is associated with a high rate of severe hypoglycemia in most people with T1DM. The average patient has numerable numbers of episodes of asymptomatic hypoglycemia and suffers two episodes of symptomatic hypoglycemia per week (with thousands of such episodes over a lifetime of diabetes). Diabetic patients suffer from one or more episodes of severe, temporarily disabling hypoglycemia, often accompanied with seizure or coma, per year [14]. Hypoglycemia remains a significant barrier to achieving lower levels of glycated hemoglobin (HbA1c). Less than 57% of individuals with T1DM are achieving target HbA1c levels [15-18]. Even with the currently available sophisticated insulin pumps and continuous glucose monitoring devices, the majority of patients with diabetes struggle to achieve optimal glycemic control. The most advanced recent technology (an artificial pancreas or a closed-loop insulin delivery system) is still under development and faces various physiological challenges and technical issues, including variability in insulin requirement, delay in insulin action and alterable accuracy of glucose sensors [19].

These observations encourage researchers to explore alternative methods of restoring physiological blood glucose regulation. Beta-cell replacement is the only treatment that reestablishes and maintains long-term glucose homeostasis with near-perfect feedback controls [20]. Whole pancreas transplantation and pancreatic islets transplantation are effective beta-cell replacement therapies for diabetic patients with negative stimulated C-peptide (≤0.3 ng/ml) [21]. Islet transplantation has recently emerged as a minimally invasive alternative to restore normoglycemia in diabetic patients. Islet transplantation is preformed by an infusion of islets via microembolization into the hepatic portal venous system. The islets entrapping occurs in its peripheral branches, at presinusoid level because of the size restriction followed by their engraftment and neovascularization from the hepatic vasculature. Once lodged in the vessels branching from the portal vein, the islets have direct contact with blood, which enables them to continuously detect blood sugar levels and, at the same time, to receive continuous nourishment [22-26].

The first successful islet transplantation was performed in 1972 when the Lacy's research group demonstrated that intraperitoneal transplantation of pancreatic islets ameliorates the effect of chemically-induced diabetes in rats [27]. Kemp demonstrated that the liver was the most physiological environment for islet implantation in rodents, because normally insulin from the pancreatic beta-cells is secreted directly into the portal venous system [28]. Najarian performed the first successful clinical islet allotransplant in 1977 [29]. In 1979, Largiader reported the first C-peptide-negative diabetic patient to achieve insulin independence at one year after a simultaneous kidney and islet transplantation [30].

However, of the 237 well-documented allotransplants in T1DM patients recorded in the Islet Transplant Registry (ITR) database in Giessen, Germany between 1990 and 1999, less than 12% of recipients were insulin-free at 1 yr posttransplant. Graft survival, defined as basal C-peptide higher than 0.5 ng/mL, was 41% [31]. The limited success of early clinical islet transplants revealed that conventional immunosuppressants were relatively ineffective in preventing allograft rejection. Most, if not, all the immunosuppressive agents were associated with impaired beta-cell function, reduced graft revascularization, or serious long-term side effects such as nephrotoxicity and malignancy [32, 33].

In 2000, Shapiro's group introduced the "Edmonton protocol", a new glucocorticoid-free immunosuppressive regimen comprised of daclizumab, sirolimus, and tacrolimus [24]. In their study, all seven patients became independent from exogenous insulin therapy once sufficient numbers of islets were transplanted. Patients required up to 3 subsequent islet transplantations from multiple donors in order to obtain a sufficient quantity of beta-cells, as certain amount of islets was lost during the early posttransplant period. The remaining islets were well protected by the new immunosuppressive therapy and allowed 100% insulin independence at 1 year posttransplant [24]. Subsequent studies confirmed that long-term insulin independence was possible and that this therapy was safe and well tolerated [34-37].

During the last decade, the immunosuppressive protocol and islets isolation technique were further improved, so the recipients who received islet grafts after 2005 retained insulin independence significantly longer than those transplanted between 1999 and 2004 [38, 39]. The Collaborative Islet Transplant Registry (CITR) included data on 571 allogeneic islet transplantation recipients (481 islet transplantations alone and 90 islet transplantations after or simultaneously with kidney transplantations), who received 1,072 infusions from 1,187 donors during 1999-2009 [39]. Overall, non-stratified achievement of insulin independence was 65% in the first year post the first infusion (with or without reinfusion). Nevertheless, the proportion of patients that was insulin independent without reinfusion (utilizing islets from a single donor) remained low, at ≈30% throughout the first year and ≈18% at 5 years post-transplantation, respectively [39]. For islet transplantations to become a widespread clinical reality, diabetes reversal should be achieved with a single donor to reduce risks and costs and increase the overall availability [38, 40].

4.3 Barriers to Successful Clinical Islet Transplantation

Long-term insulin independence after a single-donor islets infusion is the ultimate goal of transplantation studies [38, 40, 41]; however, a sufficient number of islets derived from two or more donor pancreas are usually required to achieve insulin independence. The need for multiple donors is a serious drawback given the prevalence of diabetes and the limited cadaveric organ donor pool [37]. Also, the risks associated with islet transplantation appear to increase with the number of infusions and with the total packed cell volume of cumulative grafts [42]. Islet function and wellbeing are already undermined by stressful events before transplantation [43, 44]. Donor characteristics such as medical history, glucose control, age, length of hospitalization, and cause of death have a significant impact on islet recovery after isolation [43]. During pancreas procurement and preservation, islets are exposed to warm and cold ischemia that may impair survival and eventually contribute to graft failure after transplantation [45, 46].

The isolation process is designed to remove the exocrine part of the organ while preserving structurally intact islets [47]. During isolation and purification, islets are exposed to mechanical, enzymatic, osmotic, and ischemic stresses, so a large proportion of islets can be either compromised or destroyed [48, 49]. Islet isolation triggers a cascade of events leading to apoptosis, necrosis and the production of proinflammatory molecules, which reduces islet yield and affects islet functioning after transplantation [50]. Oxidative stress plays a major role in triggering the death of islets and surrounding exocrine tissue during isolation [51]. Islet beta-cells are highly susceptible to oxidative stress because of their reduced levels of endogenous

antioxidants [52-54]. Under conditions of stress, the islet antioxidant systems may become depleted, leading to a state of redox imbalance and the production of reactive oxygen species (ROS). Isolation not only disrupts the internal vascularization and innervation of islets, but also fundamentally changes interactions between islet cells and macromolecules of the extracellular matrix (ECM). Signaling interactions between islet cells and ECM are known to regulate multiple aspects of islet physiology, including survival, proliferation, and insulin secretion [55]. During isolation, loss of islets occurs to some extent due to the activation of an anoikis-type mechanism evoked by disruption of the surrounding ECM [44, 56]. Cells disrupted from their ECM display a loss of transmembrane integrin signaling [57]. Evidence suggests that the beta-cell phenotype is fragile and easily lost upon removal of these cells from their native environment [58, 59]. The beta-cell specific transcriptional network is affected during the isolation process, and *in vitro* culture further induces de-differentiation of mature beta cells towards pancreatic progenitor cell stage [60, 61].

Early graft failure remains an important clinical problem in intraportal islet transplantation. Pancreatic islets are highly vulnerable during the immediate post-transplantation period. Experimental studies demonstrate that the most marked decrease in the islet cell mass takes place in the first 15 days after islet transplantation and persists even after revascularization has occurred [62, 63]. Post-transplantation metabolic data suggest that 25-75% of the islets fail to engraft, increasing the number of islets required to achieve initial normoglycemia after transplantation [34, 35]. Experimental models of syngeneic islet transplantation demonstrated that 60% of transplanted islet tissue was lost 3 days after transplantation due to necrosis and apoptosis [64], suggesting the involvement of nonalloantigen-specific, inflammatory events in partial destruction of the graft [65]. The rate of apoptosis following islet transplantation is 10 times higher than the rate seen in the native pancreatic islets [64].

The loss of islets during the immediate post-transplantation period is mainly due to inflammatory events, which occur before adaptive immunity initiates rejection. These include the activation of platelets, coagulation and complement systems, generation of cytokines and free radicals, recruitment of immune cells and induction of the stress response. Innate immunity and heat shock response are believed to be among the most important factors that can affect the early islet loss. The main functions of innate immunity include initiation of instant defensive reaction against foreign objects and antigen presentation [64, 66, 67].

An important mediator of inflammation in the hepatic sinusoids is the Kupffer cell, which is the resident macrophage of the liver [68]. When activated, Kupffer cells release free radicals and secrete inflammatory cytokines [69]. During stress and hypoxia islets can produce and release cytokines that attract and activate macrophages [70-72]. In addition, Kupffer cells can be activated by ischemia-reperfusion injury to the sinusoidal endothelial cells [73] and the liver parenchyma [74]. When transplanted along with pancreatic islets, acinar tissue undergoes necrosis [75], which can also contribute to Kupffer cells activation [65].

Upon injection into the recipient, direct exposure of human islets to blood triggers instant blood-mediated inflammatory reaction (IBMIR), characterized by activation of coagulation and complement systems, platelet aggregation, and infiltration of islets with neutrophils and monocytes [76-80]. IBMIR ultimately results in lysis of islet cells [81,82].

Another reason for graft failure is the absence of established vasculature, which is normally destroyed during the isolation process [63, 83]. The islets of Langerhans constitute 1-2% of

pancreas mass. However, they receive 10-20% of pancreatic arteriolar flow, demonstrating a significant need for oxygen and nutrients for immediate insulin secretion in response to glucose stimulation [84, 85]. During the first several weeks post-transplantation, the pancreatic islets are exposed only to portal venous blood [86]. The essential nutrients and oxygen can only be supplied through diffusion from the surrounding tissues into the transplanted islets [87-89]. The time required for revascularization of transplanted islets is approximately two weeks [90-92]; therefore, hypoxia is a serious contributor to islet loss in the early post-transplant period [93]. Although tissue ischemia alone may be deleterious, the reintroduction of oxygen after reperfusion is more harmful [94]. Molecular oxygen is the source of reactive oxygen metabolites, which are responsible for the majority of the tissue damage seen during the sequence of ischemia and reperfusion [95, 96].

Alloreactive T-cell-mediated graft rejection of pancreatic islets presents the major challenge in transplantation. A substantial fraction of islet transplants undergo chronic failure due to immune rejection, despite the use of modern immunosuppressive agents [97, 98]. Rejection is initiated when recipient CD4+ T cells detect donor antigens derived from a highly polymorphic region of the genome called the major histocompatibility complex (MHC). Activated CD4+ T cells contribute to the rejection process by secreting lymphokines and stimulating macrophages, CD8+ cytotoxic T cells and alloantibody-producing B cells [99].

There is also considerable evidence that immunosuppressive drugs used to prevent graft rejection have deleterious effects on beta-cell survival and/or function [100]. FK506 (tacrolimus) can inhibit glucose-stimulated insulin release and beta-cell regeneration [101]. Rapamycin (sirolimus) has been shown to have deleterious effects on beta-cell function and growth [102]. Mycophenolate mofetil (MMF) inhibits insulin secretion from islets and can induce apoptosis in beta-cells [101].

Furthermore, the grafted islets are also exposed to the autoimmune process that initiated the original disease. Pathogenic T cells and autoantibodies preexist in T1DM patients; therefore, islets transplanted to a recipient with T1DM represent a cellular transplant to a pre-sensitized host [103]. Progressive islet graft failure occurs significantly earlier in autoantibody-positive than in autoantibody-negative T1DM recipients of intrahepatic islet allografts [104].

Strong experimental evidence indicates that constant exposure of pancreatic islets to high glucose results in impaired glucose-stimulated insulin secretion and beta-cell damage [105], [106-111]. Animal studies have demonstrated that severe hyperglycemia impairs graft function, and that successful islet transplantation depends on the degree of hyperglycemia in the recipient [62, 112-117]. Labile blood sugars and chronic hyperglycemia may drive a systemic inflammatory response that creates an environment hostile to islet engraftment [117-119]. An elevated level of apoptosis was shown in pancreatic islets exposed to chronic hyperglycemia immediately after transplantation [64].

Despite the challenges listed above, the majority of recipients of pancreatic island grafts benefit from a reduced overall insulin requirements, improved C-peptide secretion and HbA1C levels, a fewer microvascular complications, and a fewer complications related to episodes of hypoglycemia after 5-year follow up [120].

4.4 Monitoring of the Islet Graft

Regardless of the islet damage pathway, there is a need to monitor surviving grafts in diabetic patients. There is no agreement on the best ways to assess islet graft function. The current clinical trials rely on metabolic monitoring of the islet graft. Overall function of transplanted islets is evaluated by measurements of plasma glucose, insulin, C-peptide, HbA1c, fructosamine levels, insulin requirement, and by calculations of the secretory unit of islet transplant objects and the beta-score. Blood glucose stability is reflected by mean amplitude of glycemic excursions, lability index and continuous glucose monitoring systems. Islet response to a standardized stimulus is assessed by an arginine stimulation test, a glucagon stimulation test, a mixed meal tolerance test, an oral glucose tolerance test, an intravenous glucose tolerance test, and a glucose-potentiated arginine stimulation test [121]. Metabolic tests are time consuming and cumbersome to perform; their use is limited to selected time points during the follow-up. Therefore, they detect graft dysfunction when a substantial islet mass has been already lost, preventing timely rescue interventions [122]. At most institutions, routine abdominal color Doppler ultrasound is performed at the time of the procedure, in the early postoperative period, and annually thereafter to allow detection of complications such as hemorrhage, portal vein thrombosis, periportal hepatic steatosis, and the presence of ischemic/necrotic regions in the recipient's liver [26]. Computerized tomography (CT) and MRI have also been used to detect intrahepatic posttransplant structural changes [123-125]. None of these imaging modalities visualize the graft directly, and various processes, including excess glycogen accumulation, edema and inflammation can affect their results. The association between graft function and liver steatosis was highly controversial because despite the presence of steatosis, graft function at the time of imaging was not compromised [126]. The only direct functional assessment of transplant fate currently available is performed through liver biopsy, which is an invasive procedure with several complications [127]. Moreover, the quantity of islets engrafted in the liver is very low and percutaneous needle biopsies have low chances of sampling islets, unless multiple biopsies are performed [121]. Development of new, non-invasive methods to determine islet graft function and the beta cell mass over time will be particularly helpful for the monitoring of islet engraftment, islet cell plasticity, and functionality after transplantation. They may also be helpful for guiding timely interventions to prevent loss of the islet mass [122].

Molecular imaging is a rapidly developing biomedical research discipline, which utilizes specific molecular probes as the source of image contrast [128, 129]. Extensive research has been done towards the development of noninvasive, high- resolution *in vivo* imaging technologies including optical imaging, nuclear imaging, and MRI. Isolated islets can be labeled before transplantation using various approaches, including genetic modification with fluorescent or bioluminescent reporters for optical imaging, labeling with exogenous contrast agents, such as superparamagnetic iron oxides for MRI, or radiolabeled metabolites for nuclear imaging [130].

The small islet size (50–300 μm) and large distribution area in the liver make noninvasive islet imaging very challenging. In order to detect a single islet in the liver, the imaging modality should have high resolution and/or employ a specific islet- or beta-cell labeling technique. Furthermore, the decrease of signal intensity must be observed earlier than the alteration of the usual graft function parameters, so the graft could be saved in the case of allograft rejection. Finally, to be approved for human clinical practice, an imaging technique must be safe both for the recipients and the islet graft [131].

The first animal studies of the noninvasive imaging of transplanted islets utilized the bioluminescence (BLI) optical imaging modality [132-136]. *In vivo* optical imaging uses light as a source of contrast. Bioluminescent cells are modified to express the luciferase enzyme gene, either after *in vitro* islet transfection with a viral vector [134], or by generating transgenic mouse strains expressing the luciferase gene under the regulation of the insulin promoter [137]. Luciferase expression does not adversely affect islet metabolic function [134, 137]. For imaging, the luciferase substrate, injected just before the image acquisition, is oxidized by luciferase in luciferase-expressing cells in an oxygen- and ATP- dependent manner [131]. The product of the reaction emits light that can be detected by a cooled charge-coupled device and quantified *in vivo* for at least 18 months [138]. There is a linear relationship between the amount of islets transplanted and the intensity of the luminescent signals detected [134]; however, the resolution of the signal is low and does not allow detection of single islets scattered throughout the liver [139]. Remarkably, luminescence intensity started to decrease several days before permanent recurrence of diabetes and histologically demonstrated acute rejection in an allogeneic model [138]. As a drawback, the light attenuates very strongly when it propagates through the tissue before reaching the detector; for that reason BLI can only be used as a research tool in mice [129, 131].

Fluorescence optical imaging employs fluorophores, which re-emit light when stimulated with light of the appropriate wavelength. A cooled charge-coupled device collects emission light from fluorophore-labeled molecules of interest distributed in biological systems. The fluorescent proteins can be visualized in both live and fixed cells/tissues, and no substrate is required for their visualization. Certain disadvantages include difficulties in quantitation, as well as the surface-weighted nature of the image in which objects closer to the surface will appear brighter than deeper structures [140]. Fluorescence optical imaging has been used for the monitoring of immunological effects associated with islet transplantation at cellular level. Bertera et al. engineered a transgenic mouse expressing proinsulin II tagged with a live-cell fluorescent reporter protein, Timer. The Timer protein has ability to change color from green to red in the first 24 h after synthesis. With this marker, insulin synthesis can be monitored with a confocal microscope through the changes in fluorescence over time. Islets expressing the Timer protein were transplanted under the kidney capsule of the recipient mice, and a body window device was inserted to monitor beta cells and migrating to the islets T cells labeled with a fluorochrome distinguishable from the Timer protein [141]. Recently, Fan et al. established methods to longitudinally track islet allograft-infiltrating T cells in live mice by endoscopic confocal microscopy and to analyze circulating T cells by *in vivo* flow cytometry. A new reporter mouse model was developed, whose T cell subsets express distinct, ‘color-coded’ proteins enabling *in vivo* detection of different T-cell subsets. Marked differences were observed in the T cell response in islet grafts recipients receiving tolerance-inducing treatment compared to control group [142]. These studies established a real-time cell-tracking tool for monitoring islet graft rejection, but they lack an equivalent applicable to human studies, thus preventing their direct translation to clinical use.

Positron emission tomography (PET) is a nuclear imaging technique that provides high resolution, good sensitivity, and accurate quantification of physiologic, biochemical, and pharmacologic processes in living subjects [131]. For the last decade PET has been employed for pre-clinical and clinical imaging of islet transplantation. PET imaging utilizes positron-emitting radioisotopes (tracers) as labels. Radioactive probe, containing a biologically active molecules tagged with a tracer, can be introduced into the subject and then PET imaging can follow their

distribution and concentration over time [143]. Large animal [144] and clinical [145, 146] studies on hepatic grafts employed the commonly used 18F-fluorodeoxyglucose (18F-FDG) probe for pre-transplant labeling of isolated islets. 18F-FDG enters the cell by the same transporters as glucose and is rapidly phosphorylated ensuring high intracellular retention [147]. Following intraportal infusion 18F-FDG-labeled islets appeared as multiple "hot spots" heterogeneously distributed throughout the liver. On average, only 63% of the administered radioactivity was detected in the liver, suggesting that considerable amount of transplanted islet cells were damaged to the extent that the 18F-FDG they contained was released during the first few minutes after transplantation. A parallel, marked increase in plasma C peptide was observed, also indicating islet destruction presumably due to IBMIR. Clinical outcome in all patients was comparable to that previously observed indicating that the 18F-FDG labeling procedure did not harm the islets [145, 146]. However, because of the short half-life of 18F (109.8 min), this technique can be used only to study islet survival and engraftment immediately after islet infusion. If the same technique could be used with an isotope with markedly longer radioactive half time to allow imaging over several days to weeks, possible damaging radiation effects on the islets would have to be investigated in further detail before clinical use [146]. Another type of PET tracer 18F-FHBG has been used for tracking mouse islets transfected with a mutant form of the gene encoding for herpes simplex virus 1 thymidine kinase (HSV1-sr39tk) in a series of studies [148-151]. 18F-FHBG accumulations at the transplantation sites were linearly correlated with the size of the engineered graft. However, tracer uptake at the graft site declined over the following several weeks, which was partially related to the transient nature of adenovirus-directed gene expression. Genetic engineering of islets prior to administration can be damaging, and development of safer and more controllable gene transfer systems may be required before translation into clinical islet transplantation [152]. A novel PET probe 64Cu-DO3A-VS-Cys40-Exendin-4 targeting glucagon-like peptide 1 receptor (GLP-1R) on beta-cells has been tested for detecting of human islets transplanted into the mice liver [153]. Ten days after transplantation, liver uptake of the radiotracer was significantly higher in transplanted mice than in control mice. Further studies are needed to test the feasibility of long-term monitoring of transplanted islets with 64Cu-DO3A-VS-Cys40- Exendin-4.

Magnetic resonance imaging is one of the most reasonable modalities to explore for tracking of pancreatic islets following transplantation. MRI does not utilize ionizing radiation, has tomographic capabilities, can deliver the highest-resolution images *in vivo*, and has unlimited depth penetration. Tissue contrast in MR images reflects the differential distribution of hydrogen (^{1}H) atoms in particular tissues. As hydrogen atoms (protons) are mainly found within water molecules, MRI scans essentially visualize the distribution of water molecules in different types of tissues. This relative distribution varies among tissues, and there are other macromolecules (i.e., proteins) that can contain bound water in various amounts. In addition, protons can be found in chemically distinct substances, such as lipids (e.g. myelin and adipose tissue), and paramagnetic endogenous tissue iron can also be found in certain tissues. All these factors determine contrast between tissues [154]. MRI is routinely used for the morphologic evaluation of structural changes in the liver after islet transplantation [126]. However, this method has not been reported to be able to visualize native or transplanted pancreatic islets, most likely because their magnetic properties are similar to the surrounding tissue. Therefore, a contrast agent must be applied in order to visualize islets on MR images.

Superparamagnetic iron oxide nanoparticles have been extensively used as magnetic resonance reporters for detecting pathologies in different organs [155]. The basic structure of these

nanoparticles includes an iron oxide core covered with a dextran coat [156] that can be further modified depending on the need of the specific study. Nanoparticle presence in tissue is evident primarily by a darkening effect on T2-weighted MR images. Remarkably, the T2* effect of superparamagnetic iron oxides results in a hypointensity footprint many times larger than the labeled entity, in essence constituting a powerful signal amplification tool. With its high spatial resolution and the fact that physiologic and anatomic information can be extracted simultaneously, MRI is now capable of providing high-resolution images (on the order of tens of microns per voxel resolution) of nanoparticle disposition *in vivo*, both in small animals and in humans [157]. Our laboratory pioneered studies on imaging of the diabetic pancreas including imaging of autoimmune attack ex vivo [158] and in vivo [159], imaging of beta-cell mass [160] and beta-cell death [161]. Taking into account its importance and potential clinical use in the near future, *in vivo* magnetic resonance imaging of pancreatic islet transplantation has been one of the major directions of our research.

5. Aims of the Thesis

The main objective of this work was to develop and evaluate a method to non-invasively detect human pancreatic islets, labeled with an MRI contrast agent, and transplanted into diabetic animals.

The specific aims were to investigate:

- whether human pancreatic islets could be labeled with a magnetic imaging probe that would produce a sufficient signal-intensity change on magnetic resonance images without altering islet insulin-producing function
- whether labeled islets can be monitored *in vivo* by MRI noninvasively and repeatedly in real time
- whether the relative transplanted islet mass can be quantified and tracked over time by MRI
- whether MRI can monitor islet death due to immune rejection or glucose toxicity noninvasively and repeatedly in real time.
- whether islet purity has any effect on labeling by a magnetic imaging probe
- whether MRI of labeled pancreatic islets can be applied to a non-human primate model

6. Materials, Methods, and Results

6.1 Paper I and Paper II (Methods only). In Vivo Imaging of Pancreatic Islet Transplantation

<u>Study design:</u> Human pancreatic islets labeled with magnetic nanoparticles modified with the near-infrared fluorescent Cy5.5 dye (MN-NIRF)

Aims / Details of the Study	Imaging Modality/ Assay	Main Results
Part 1. In Vitro Islet Analysis		
Labeling of isolated islets with MN-NIRF	Fluorescence microscopy (near-infrared channel) of isolated islets	All islets in the field of view appeared to be labeled with the probe (Fig. 1a). Control unlabeled islets did not have any signal.
Magnetic resonance imaging of labeled islets	MRI 9.4T of islet phantoms	Labeled islets caused a marked decay in tissue transverse magnetization (T2/T2* effect) on MRI. The signal intensity of labeled islets decreased compared to unlabeled islets, and these labeled islets appeared hypointense (dark) as a result of MN-NIRF accumulation (Fig. 1b)
Correlation between number of islets and change in T2/T2* relaxivity	MRI 9.4T of islet phantoms	There was a direct linear correlation between T2* values and number of labeled islets (Fig. 1c).
Iron uptake per islet cell after incubation with increasing concentrations of the MN-NIRF probe	Total Iron Reagent Set	Iron uptake by the islets varied from 2.26 ± 0.53 to 12.17 ± 0.97 pg iron/cell (Fig. 1d) (assuming 2,000 cells/islet).
Staining of labeled islet sections for an endosomal marker (CD71)	Confocal microscopy	The majority of Cy5.5 in the islet cells was associated with intracellular endosomal staining, indicating its intracellular localization (Fig. 1e, Supplementary Fig. 1).
Electron microscopy of labeled islets	Transmission electron microscope	Confirmed the intracellular localization of the probe linked to endosomal structures (Supplementary Fig. 2).

Staining of labeled islets with antibodies targeting: insulin-, somatostatin- and glucagon-producing cells	Triple-channel immunofluorescence microscopy	The Cy5.5 signal colocalized mainly with insulin-specific staining, suggesting that the majority of the MN-NIRF probe associated with beta cells (Fig. 1f).
Insulin secretion by labeled islets	ELISA	Labeling with MN-NIRF does not affect islet insulin function.
Viability of labeled islets	MTT	Islet viability remained unchanged.
Part 2. MN-NIR-Labeled and Unlabeled Islets Transplanted under the Left and Right Kidney Capsule of Healthy Nude (nu/nu) Mice		
Feasibility of magnetic resonance imaging of islets *in vivo*	MRI 4.7T	Decrease in signal intensity on T2* MRI images at the implantation site of labeled islets was observed up to 188 days (Fig. 2a). Analysis of T2 maps showed a significant difference in T2 relaxation times between labeled and unlabeled grafts for the duration of the experiment (Fig. 2b and Supplementary Fig. 3).
Detection threshold of magnetic resonance imaging of islets *in vivo*	MRI 4.7T	The T2 relaxativity depended on the number of transplanted islets. There was a direct linear correlation between the number of islets in the graft and graft volume (Fig. 2c).
In vivo imaging of the labeled islet graft	Near-infrared optical imaging of the mouse	A bright fluorescent signal at the transplantation site indicated the presence of labeled islets in the kidney (Fig. 3a).
Ex vivo imaging of excised kidneys	Near-infrared optical imaging	Imaging confirmed the presence of fluorescent signal coming from the labeled graft and the absence of fluorescence in the unlabeled graft (Fig. 3b).
Staining of the graft sections for an endosomal marker (CD71)	Confocal microscopy	Colocalization of the probe with endosomes indicated that after transplantation the probe maintained its intracellular localization within the graft after *in vitro* labeling (Fig. 3d and Supplementary Fig. 6).
Staining of the graft sections for insulin	Triple-channel fluorescence microscopy	Pancreatic islets within the graft maintained their ability to secrete insulin 188 d after transplantation (Fig. 3e).
Staining of the graft sections for apoptosis	TUNEL assay	The amount of apoptosis in the graft 188 days after transplantation was negligible (Fig. 3f). No evidence of massive islet cell death that could result in the release of substantial amounts of iron, which would create 'false-positive' T2 measurements.

Part 3. MN-NIRF-Labeled and Unlabeled Islets Transplanted Under the Kidney Capsule in Streptozotocin-treated Nonobese Diabetic–Severe Combined Immunodeficient (NOD-SCID) Mice		
Restoration of normoglycemia	Glucometer	Seven to ten days after transplantation, mice became euglycemic for the duration of the experiment. There was no difference in achieving normoglycemia between mice transplanted with labeled and unlabeled islets.
In vivo imaging of labeled islets	MRI 4.7T	Considerable darkening was observed at the site of labeled islet transplantation in the kidney (Fig. 2d). T2 maps confirmed that the nature of the signal observed in the kidney owed to the presence of the labeled graft (Supplementary Fig. 4).
Ex vivo imaging of excised kidneys	Near-infrared optical imaging	A bright fluorescent signal at the transplantation site indicated the presence of labeled islets in the kidney (Supplementary Fig. 5).
Ex vivo imaging of excised kidney cross-sections.	MRI and optical imaging	Confirmed that the signals obtained with both modalities originated exclusively from the graft (Fig. 3c).
Part 4. MN-NIRF–Labeled and Unlabeled Islets Transplanted Intraportally in Streptozotocin-Treated Nonobese Diabetic–Severe Combined Immunodeficient (NOD-SCID) Mice		
Feasibility of *in vivo* imaging of labeled islets	MRI 4.7T	Labeled islets appeared as dark hypointense spots representing single islets and/or islet clusters (Fig. 4a). Unlabeled islets could not be detected.
Longitudinal monitoring of transplanted islets	MRI 4.7T	Labeled islets were readily visible for the duration of the experiment. The overall associated $T2^*$ values increased somewhat and then reached a plateau over time (Fig. 4a), possibly indicating islet loss in this initial post-transplant period.
Restoration of normoglycemia	Glucometer	Normoglycemia in diabetic mice transplanted with labeled or unlabeled islets was restored within 1 week.
Ex vivo imaging of excised liver	Near-infrared optical imaging	Bright foci represented transplanted islets and thus confirmed the presence of the probe in the graft (Supplementary Fig. 7).
Correlative microscopy of liver sections (H&E, Cy5.5, insulin).	Bright light and fluorescence microscopy	Studies confirmed the presence of labeled islets in the liver and their ability to secrete insulin (Fig. 4b).

Conclusions:

- Human pancreatic islets can be labeled by superparamagnetic iron oxide nanoparticles (MN-NIRF)

- Labeling of human pancreatic islets with MN-NIRF does not adversely affect islet viability and function

- The MN-NIRF-labeled pancreatic islets transplanted under the mouse kidney capsule or into the mouse liver appear as dark hypointense foci representing islet clusters and/or single islets on T2*-weighted images

- There is a direct linear correlation between T2* values and a number of the labeled islets

- MRI can be used to monitor labeled pancreatic islets *in vivo* noninvasively and repeatedly in real time

6.2 Paper III. In Vivo Imaging of Immune Rejection in Transplanted Pancreatic Islets

<u>Study design:</u> Human pancreatic islets labeled with the FDA-approved, commercially available superparamagnetic iron oxide nanoparticle-based contrast agent Feridex (ferumoxide).

Aims / Details of the Study	Imaging Modality/ Assay	Main Results
Part 1. In Vitro Islet Analysis		
Iron uptake per islet cell after incubation with increasing concentrations of Feridex	Total Iron Reagent Set	Iron uptake by the islets varied from 1.21 ± 0.36 to 18.26 ± 1.36 pg iron/islet cell, (assuming 2,000 cells/islet) (Fig. 1B).
Time course study of iron uptake by the islets	Total Iron Reagent Set	There was an increase in the islet iron content with increasing incubation time, with a maximum at 12 h (Fig. 1C).
Feridex retention by the islets	Total Iron Reagent Set	The iron content of islets remained constant after incubation in Feridex-free culture for up to 24 h (Fig. 1D).
Amount of Feridex accumulated in islets	Prussian Blue stain and Light microscopy	The accumulation of Feridex in islets varied from 10 to 70% (Fig. 2B).
Feridex distribution in islet cells: islets were stained for insulin, glucagon, somatostatin, macrophages and iron	Immunohistoche-mistry, Prussian Blue stain and light microscopy	Feridex colocalized with insulin-producing beta-cells andm, to a lesser degree, with delta, alfa cells and resident macrophages (Fig. 2A).
Insulin secretion and viability of Feridex-labeled islets	ELIZA and MTT	Insulin secretion and islet viability after exposure to Feridex remained unchanged.
Magnetic resonance imaging of labeled islets	MRI 9.4T of islet phantoms	Labeled islets produced a decrease in signal intensity on T2-weighted images (Fig. 1A).
Part 2. Feridex-Labeled Islets Transplanted Intraportally in Severe Combined Immunodeficient (NOD-SCID) and Immunocompetent (Balb/C) mice. Control Animals Transplanted with Unlabeled Islets.		
In vivo imaging of transplanted islets	MRI 4.7T	Islets transplanted into the liver appeared as dark hypointense foci representing single islets and/or, possibly, islet clusters (Fig. 3A), whereas unlabeled islets did not cause any change in signal intensity on T2*-weighted images (Fig. 3B).

Analysis of the relative transplanted islet mass on MR images Validation of the method by creating a calibration curve	MRI 4.7T Manually scoring of the signal voids on MR images	The known number of transplanted islets directly correlated to the number of dark voids representing labeled islets/islet clusters found on T2*-weighted images (Fig. 3D).
Visual co-registration of matching slices on MR images of immunocompetent and immunocompromised mice	MRI 4.7T	Disappearance of signal voids in Balb/c mice was more pronounced than in NOD.scid mice over time (Fig. 3C).
Islet loss in immunocompetent and immunocompromised mice	MRI 4.7T The number of signal voids on MR images was scored manually	Immunocompetent mice exhibited a significantly higher rate of islet disappearance compared with immunocompromised animals, especially pronounced on day 10, and resulting in a 20% difference in islet number by 14 days after transplantation (Fig. 3E).
Part 3. Livers from the Animals Excised on Each Day of Imaging and Used for Ex Vivo Studies.		
Immune rejection of transplanted islets. Staining with antibodies targeting: helper-inducer T-cells (CD4), cytotoxic/suppressor T-cells (CD8), B-cells (CD19), monocytes/ macrophages (CD68), neutrophils	Immunohistoche-mistry and light microscopy	Infiltration of the graft by CD68, CD4, CD8, CD19 positive cells and neutrophils in Balb/c mice started on the first day after transplantation (Table 2, Fig. 4A). The level of infiltration by these cells increased with time and peaked on days 10-11 in agreement with the TUNEL assay results. In contrast, NOD.scid mice showed only marginal presence of immune cells in islets after transplantation except for CD68 positive invading macrophages (Fig. 4B).
Apoptosis rate in transplanted islets	TUNEL staining and fluorescence microscopy (near-infrared channel)	In NOD.scid and Balb/c mice apoptosis was most pronounced on day 1. The number of apoptotic cells in immune-deficient mice decreased to 1.8% by day 4 and stayed at this level for the duration of the study. In contrast, the number of apoptotic cells in immunocompetent mice gradually decreased to 3.3% on days 4-5 followed by severe antigen-specific rejection, which destroyed up to 13.2% of the islets on days 10-11 (Fig. 3E). The apoptosis level gradually decreased by day 14 since by that time, almost all cells in the islets were destroyed.

Fate of Feridex in transplanted islets after islet death	Prussian Blue stain and Light microscopy	After death islets released Feridex into the liver parenchyma where it was internalized and processed by Kuppfer cells. (Fig. 5C).

Conclusions:

- Human pancreatic islets can be labeled with the Food and Drug Administration–approved, commercially available contrast agent Feridex
- Labeling of human pancreatic islets with Feridex does not adversely affect islet viability and function
- The Feridex-labeled islets transplanted into the mouse liver appear as dark hypointense foci representing single islets and/or islet clusters on T2*-weighted images
- In the mouse transplantation model, the relative transplanted islet mass can be quantified by manually scoring the number of hypointense voxels representing islet graft on MR images. The islet mass value can be tracked over time
- MRI can monitor islet death due to immune rejection noninvasively and repeatedly in real time

6.3 Paper IV. Effects of Glucose Toxicity and Islet Purity on In Vivo Magnetic Resonance Imaging of Transplanted Pancreatic Islets

<u>Study design:</u> Human pancreatic islets labeled with the FDA-approved, commercially available superparamagnetic iron oxide nanoparticle-based contrast agent Feridex (ferumoxide).

Aims / Details of the Study	Imaging Modality / Assay	Main Results
Part 1. Islets of 20% and 98% Purity Labeled with Feridex		
Iron uptake by islets expressed as iron-to-protein ratio	Total Iron Reagent kit / Protein assay	Iron uptake was significantly higher in high-purity islets than in low-purity islets (Fig. 3A).
Part 2. Pure Islets and Non-endocrine Tissue Labeled with Feridex		
Imaging of Feridex-labeled and unlabeled high-purity islets, non-endocrine tissue and islets mixed with non-endocrine tissue.	MRI 9.4T of cell phantoms	Labeled islets had T2 values significantly lower than the labeled non-endocrine tissue and a 67%/33% mixture of labeled islets and non-endocrine cells.
Part 3. Feridex-Labeled Islets of 95% and 50% Purity Transplanted Intraportally in Healthy and Severe Combined Immunodeficient (NOD-SCID) Mice		
In vivo magnetic resonance imaging of transplanted islets of different purity	MRI 4.7T	Visually, the number of dark spots representing labeled islets appeared to be the same (Fig. 4A,B).
Quantitative analysis of islet loss on MR images	MRI 4.7T	The two groups of animals did not exhibit any statistically significant difference in islet disappearance rate throughout the study (Fig. 5A).
Ex vivo analysis of apoptosis rate in transplanted islets	TUNEL staining and fluorescence microscopy (near-infrared channel)	Graft cell death on day 2 was 4.2-fold higher in mice transplanted with 50% purity islets than in mice transplanted with 95% purity islets (Fig. 5B).
Ex vivo analysis of graft-bearing livers for acinar and ductal elements	Immunohisto-chemistry and light microscopy	Non-endocrine tissue was detectable in both groups of animals on day 2, but was higher in quantity in 50% purity islet grafts (Table 1). The disappearance of acinar and ductal elements was more pronounced in the grafts of 50% purity.
Macrophage infiltration of islets grafts	Immunohisto-chemistry and light microscopy	Macrophage infiltration was significantly higher on days 6 and 15 in the 50% purity grafts contaminated with non-endocrine tissue (Fig. 5C).

Part 4. Feridex-Labeled Islets Transplanted Intraportally in Healthy and Diabetic Severe Combined Immunodeficient (NOD-SCID) Mice		
MR imaging of healthy and diabetic mice transplanted with Feridex-labeled islets	MRI 4.7T	There was a visual difference in number of islets between the groups on day 5 after transplantation (Fig. 1A,B).
Quantitative analysis of the number of transplanted islets in control and diabetic mice	MRI 4.7T	Half-life of the islets in diabetic mice was on average 2.6 times shorter than in healthy animal (Fig. 2A).
Glucose homeostasis	Glucometer	Before islet transplantation, blood glucose values were more than sevenfold higher in diabetic mice than in healthy animals (Fig. 2B). Diabetic mice became normoglycemic on day 10.
Correlation between the number of islets observed and corresponding blood glucose levels	Pearson correlation	In diabetic animals, newly transplanted islets experience glucotoxic stress (on Fig. 2C points with high glucose levels and high number of newly transplanted islets). Some islets died. Islets that survived restored normoglycemia (points with low glucose levels and low islet number). In the control animals, glucose levels stayed normal and had no influence on islet survival.
Ex vivo analysis of apoptosis rate in transplanted islets	TUNEL staining and fluorescence microscopy (near-infrared channel)	The apoptotic rate was higher in diabetic animals. (Fig. 2D).

Conclusions:

- MRI can monitor pancreatic islet death due to glucose toxicity noninvasively and repeatedly in real time

- Transplantation of pancreatic islets contaminated with non-endocrine tissue does not have any significant influence on MR images, presumably because of a low labeling rate of this tissue and a fast rate of its disappearance after transplantation

6.4 Paper V. In Vivo Imaging of Autologous Islet Grafts in the Liver and Under the Kidney Capsule in Non-Human Primates

<u>Study design:</u> Baboon pancreatic islets labeled with the Food and Drug Administration-approved superparamagnetic iron oxide contrast agent Feridex (ferumoxide).

Aims / Details of the Study	Imaging Modality / Assay	Main Results
Part 1. In Vitro Islet Analysis		
Insulin secretion	ELISA	Glucose-stimulated insulin release was unchanged in labeled versus unlabeled islets (Fig. 1C).
Iron retention assay	Total Iron Reagent Set	The iron content of baboon islets remained constant after incubation in a Feridex-free culture for 24 hr (Fig. 1A).
Apoptosis assay	Fluorometric caspase-3 assay	Labeling islets with Feridex did not increase the apoptotic rate in labeled compared with unlabeled islets (Fig. 1B).
Part 2. After a Partial Pancreatectomy, Feridex-Labeled Islets Autotransplanted Underneath the Renal Capsule and into the Liver of a Baboon (Papio hamadryas)		
MR imaging of islets transplanted under the kidney capsule	MRI 1.5T	On T2*-weighted MR images, islets appeared as a pocket of signal loss disrupting the contour of the kidney (Fig. 2A). Signal coming from the graft was detectable throughout the follow-up period.
MR imaging of islets transplanted intrahepatically	MRI 1.5T	On T2*-weighted MR images, islets appeared as distinct areas of signal loss, seen as signal voids dispersed throughout the liver (Fig. 2B). Signals coming from the islets were detectable throughout the follow-up period.
Development of a semiautomated image segmentation algorithm for analysis of the transplanted islet mass.	Automated segmentation method, K-means (based on MatLab)	The kidney and the liver were each classified into two labels based on their T2* values: the islet graft label and the renal parenchyma (Fig. 3A), or the islet graft label and the liver parenchyma (Fig. 3B). The T2* values associated with the two labels were sufficiently distinct to allow precise differentiation between the two in both the kidney and the liver transplantation models

Computational analysis of relative transplanted islet mass on MR images	Semiautomated image segmentation algorithm	There was a relative stability in the islet mass transplanted underneath the renal capsule during the initial (30 days) posttransplant period (Fig. 4A). In the intrahepatic model, there was a noticeable 25% decrease in transplanted islet mass between days 3 and 8 after transplantation. This was followed by stabilization of the graft over the observation period (Fig. 4B).
Long-term safety of transplanting the Feridex-labeled islets	Complete blood count, total serum protein, lipid profile, liver function tests, blood urea nitrogen and creatinine	During the follow-up the animals showed no signs of infection, anemia (Fig. 5A) or symptoms of systemic inflammation. They maintained normal weight gain and protein metabolism. The changes in triglycerides and cholesterol levels were transient and associated with the surgical transplantation procedure, with normalization thereafter (Fig. 5B). Besides a transient increase in the levels of aspartate aminotransferase, alanine aminotransferase, and bilirubin after the partial pancreatectomy, the liver function tests indicated no effects on hepatic physiology (Fig. 5C). Blood urea nitrogen and creatinine values remained within normal range during the follow-up period suggesting normal renal function (Fig. 5D).
Long-term functionality of the transplanted Feridex-labeled islets	Fasting blood glucose, intravenous glucose tolerance test	Fasting blood glucose (Fig. 6A) and intravenous glucose tolerance (Fig. 6B) remained normal and unchanged before and after completion pancreatectomy, indicating that the labeled grafts were sufficient to maintain glucose homeosta- sis.

Conclusions:

- Baboon pancreatic islets can be labeled by the Food and Drug Administration–approved, commercially available contrast agent Feridex
- Labeling of baboon pancreatic islets with Feridex does not adversely affect islet viability and function
- On T2*-weighted MR images, pancreatic islets transplanted underneath the renal capsule appear as an area of signal loss

- On T2*-weighted MR images, pancreatic islets transplanted intrahepatically appear as distinct areas of signal loss, seen as signal voids dispersed throughout the liver

- Low-field clinical MRI system can monitor pancreatic islets transplanted into non-human primates noninvasively and repeatedly in real time

- Semi-automated image segmentation algorithm can be used for the reliable identification of image voxels occupied by the graft and quantitative analysis of their relative abundance over time

- The Feridex-labeled pancreatic islets maintain their insulin secretion function and, following autologous transplantation, do not have adverse effects on the primate's health

7. General Discussion

Pancreatic islet transplantation is a promising beta-cell replacement therapy for patients with T1DM. High rates of insulin independence can be achieved shortly after transplantation; nevertheless, a majority of patients resume insulin treatment in the first 5 years after receiving the graft. Islet transplantation is still an experimental procedure and numerous studies are being directed toward optimization and modification of the current methods of islet transplantation with the ultimate goal of long-term survival of islets. Contemporary research is concentrated on the development of advanced imaging modalities to evaluate morphology of transplanted islets and monitor their mass, distribution, and function. Noninvasive imaging is essential to a more detailed understanding of the dynamics of transplantation and the complex biological aspects that determine islet graft survival [26].

MRI is emerging as a technology with a high potential for islet monitoring in the clinical setting due to its capacity for noninvasive longitudinal assessments. Furthermore, MRI has two specific advantages over PET and optical imaging: higher spatial resolution (micrometers rather than several millimeters) and the fact that physiological, molecular, and anatomical information can be obtained simultaneously. Spatial resolution is a measure of the accuracy or detail of graphic display in the images expressed in millimeters. It is the minimum distance between two independently measured objects that can be distinguished separately, or in other words, how fine the image is [162]. High field strength MRI scanners (4.7 T, 9.4 T, 15 T) with near-microscopic resolutions are now available for small animal research, and 7 T magnets are already in use in some clinical systems. In addition, MRI is a modality which does not utilize ionizing radiation, has tomographic capabilities, and unlimited depth penetration through tissues [163].

MRI is based on the principal that unpaired nuclear spins, called magnetic dipoles (such as hydrogen atoms in water and organic compounds), align themselves when placed into a magnetic field. A strong magnet in the MRI scanner produces a magnetic field around the subject under examination. There are also “coils” within the magnet to produce a gradient in this magnetic field in the X, Y, and Z axes. In addition, the magnet contains a radiofrequency coil that can produce a temporary radiofrequency pulse to change the alignment of the spins. Following the pulse, the magnetic dipoles return to their baseline orientation, which is detected (also by the radiofrequency coil) as a change in electromagnetic flux (radiofrequency waves in the range 1-100 MHz). An important function of the scanner is to determine the rate at which these dipoles relax to their baseline orientation. This measurement is translated into an MR signal. Dipoles in different physicochemical environments will have different relaxation times and thus, generate different MR signals. For example, dipoles in a lipid- or hydrocarbon-rich environment will have significantly shorter (up to 20×) relaxation times than dipoles in an aqueous environment. This is one of the main ways by which image contrast is achieved in MRI. The timing parameters of pulse excitation and recording can be altered by a central computer resulting in images with different types of magnetic contrast. The two most frequently used timing parameters are known as T1 and T2 weighting [162].

MRI is sensitive to soft-tissue differences and irregularities, but pancreatic islets do not stand out from the surrounding tissues on MR images. Incorporation of MR contrast agents into islet cells renders them distinct from the surrounding tissue and therefore allows the in vivo identification and tracking of labeled islets by MRI [154]. Superparamagnetic iron oxide (SPIO)

nanoparticles are widely used as a platform for many MRI contrast agents. Their basic structure includes an iron oxide core covered with a dextran coat that can be functionalized with additional imaging, targeting, or therapeutic moieties [156]. The presence of iron oxides in tissue is evidenced by a loss in signal intensity on T2-weighted and T2*-weighted MR images or, in technical terms, by a shortening of the T2 relaxation time of surrounding water protons [164], [130].

In our first studies, we developed a method for the noninvasive detection and monitoring of pancreatic islet grafts by dual-modality fluorescence/MRI utilizing a MR 4.7 T scanner (Paper I and Paper II). We used 30-nm SPIO magnetic nanoparticles (MNs) modified with the near-infrared fluorescent Cy5.5 dye (MN-NIRF). As a result, in addition to their magnetic properties, these nanoparticles carried fluorochromes for optical imaging. After incubation with MN-NIRF, isolated islets were associated with a bright fluorescence signal in the near-infrared channel and appeared to be labeled with the probe. Intracellular internalization of the probe by endosomes was confirmed by electron and fluorescence microscopy. Labeling of human islets with MN-NIRF did not adversely affect islet viability or islet function. MN-NIRF-labeled human islets transplanted under the mouse kidney capsule or into the mouse liver appeared as dark hypointense areas representing islet clusters and/or single islets on T2*-weighted images. There was a direct linear correlation between T2* values and number of labeled islets. MRI *in vivo* monitored labeled islets transplanted under the kidney capsule noninvasively and repeatedly in real time for up to 188 days, demonstrating graft stability and persistence of the label. We demonstrated that human pancreatic islets could be labeled with a magnetic imaging probe that could produce a sufficient signal-intensity change on magnetic resonance images without altering islet insulin-producing function. Jirak *et al.* correspondingly demonstrated the feasibility of labeling, detecting, and longitudinal monitoring of intrahepatically transplanted rat islets by a MR 4.7 T scanner. Their research group utilized a commercially available, 62 nm carboxydextran coated SPIO MNs based contrast agent Resovist (ferucarbotran). Hypointense regions in the liver were detectable on T2*-weighted images for up to 22 weeks; however, they gradually and slowly diminished over time. The hypointense areas did not noticeably change shape. They stayed homogeneously distributed throughout the whole liver and remained in the same position during the entire measurement period. Resovist-labeled islets preserved their vitality and function both *in vivo* and *in vitro* [165].

The definitive goal of our imaging research was its future clinical application for the management of patients with T1DM. For that reason, we employed a clinically relevant intrahepatic transplantation model in our subsequent studies (Paper III). For islet labeling we utilized the FDA-approved and commercially available contrast agent Feridex, which is routinely used in the clinic for liver neoplasm imaging. Similar to MN-NIRF, Feridex consists of SPIO covered with a dextran coat. When used for hepatic MRI, intravenously injected Feridex is rapidly cleared from the bloodstream by the hepatic reticuloendothelial system (Kupffer cells). The phagocytosed iron-oxide core of Feridex is broken down into other forms of iron and then incorporated normally into hemoglobin in newly formed erythrocytes [166]. In our study, labeling with Feridex did not affect islet viability or function. On MRI scans, labeled, transplanted islets appeared as distinct hypointense foci that were dispersed throughout the liver parenchyma. The relative islet mass was quantified and tracked over time by manually scoring the number of hypointense voxels representing islet graft on sequential MR Images.

We used this approach to evaluate the relative contribution of immune rejection to islet loss in the early posttransplantation period by comparing the change in the transplanted islet mass over time in immunocompetent and immunocompromised mice. The analysis showed that the number of islets in both models started to decline immediately after transplantation. This immediate decrease was consistent with islet death after transplantation due to mechanical injury, ischemia, and antigen-independent inflammatory events. The rate of islet loss gradually decreased during the course of the study and plateaued between days 10 and 14. However, immunocompetent mice exhibited a significantly higher rate of islet disappearance on MR images, in contrast to immunocompromised animals. This was especially pronounced on day 10 and resulted in a 20% difference in relative islet number by 14 days after transplantation, apparently due severe immune rejection. The MR imaging data correlated with the apoptotic rate showed by a TUNEL assay performed on excised livers. This rejection was evident from our correlative immunohistochemical studies, which confirmed that the higher rate of islet death detected by MRI and TUNEL assay in immunocompetent mice was due to significant immune cell infiltration. As a result of this study, we demonstrated that MRI could track relative mass values of intrahepatically transplanted islets over the time. MRI could also monitor islet death due to immune rejection noninvasively and repeatedly in real time. We anticipate that these studies could make a significant impact on allotransplantation and the development of new and improved immunosuppressive regiments. Immune-rejection-related islet loss was also studied in rats following islet labeling with Resovist and allogeneic or syngeneic transplantation of islets into the liver [167]. By the end of the study, 6 weeks after transplantation, rejection of the grafted allogeneic islets had resulted in a loss of 65% of the initially transplanted islet mass. In a recent study Lee *et al.* proved that pancreatic islet grafts and their rejection could be imaged on a 1.5 T clinical MRI scanner [168]. Islets were labeled by a novel magnetosome-like polyethylene glycol-phospholipid (PEG-phospholipid)-encapsulated magnetite nanocubes (FIONs). FIONs exhibited a very high relaxivity (considerably higher than Feridex) producing a strong contrast effect on a 1.5 T scanner, while the chemical composition of FIONs had similarities with Feridex. Immune rejection was studied in syngeneic and allogeneic rat models. The syngeneic islets transplanted into the liver were observed up to 150 days after transplantation, although the number and size of their hypointense spots in the T2* images progressively decreased. The number of dark spots representing allografted islets decreased significantly, even one day after transplantation. Furthermore, immunohistochemical sections of liver three days after transplantation showed that the infiltration of immune cells had already begun. The pattern of islet disappearance in allogenic rats resembled the data obtained in our study (Paper III). In addition, Lee *et al.* successfully used FIONs in a swine model of islet rejection. After the infusion, islets were observed in the T2* MR images as hypointense spots throughout the liver of animal receiving immunosuppressive therapy. On the contrary, no dark spot was shown in swine that did not receive immunosuppressive treatment [168].

We found that iron distribution within islets was not uniform ranging from 11% to 67% (Paper III). Similar findings were described by Jiao *et al*., who labeled rat islet with ferucarbotran [169]. Our previously reported observations (Paper I) and the additional immunohistochemical and Prussian Blue staining (Paper III) revealed that labeling with iron oxides involves all islet cell types. Apparently, the labeling mostly involves the beta-cells because these cells represent the largest cell population in the islet. Feridex did not have any specificity toward islet cells, and cellular uptake was most likely associated with conventional fluid phase endocytosis. Iron accumulation by islets incubated with increasing concentrations of Feridex varied from 1.21 ±

0.36 to 18.26 ± 1.36 pg iron/islet cell for Feridex (assuming 2,000 cells/islet). These levels of iron uptake correlated with data published by Berkova *et al.* [170].

Since there was a discrepancy about the fate of iron nanoparticles inside the islet cells after labeling with MNs, Berkova *et al*. investigated in detail the time behavior of the labeling process and iron accumulation in different islet cell types. Ferucarbotran particles were visualized with electron microscopy as characteristic irregular crystals with an extremely high electrodense core and a less-dense coating. After a 1-hr labeling period, ferucarbotran was found adhered on the endocrine cell surface, whereas few particles were already found in the endocytic structures of macrophages. After a 4-hr culture period, the particles were localized also in the beta-cell vesicles. With the prolonged labeling time, the amount of incorporated particles further increased and formed huge electrodense clusters. Importantly, the ultrastructure of the labeled islet cells was not affected; typical cytoplasmatic organelles and cell-to-cell contacts were observed. It had been demonstrated previously that the release of free iron from SPIO particles was dependent on buffering systems and pH [171]. Berkova *et al*. observed some endosomes that fused with lysosomes and were degraded, but the majority of particles remained unchanged in endosomes. We believe that the latter study is very important for understanding of the possible effects of SPIO nanoparticles on diverse aspects of cell activities. A potential toxic effect of SPIO on pancreatic islets has not been reported to date, and the majority of islet labeling studies emphasized the safety of SPIO based contrasts agents (Paper I, Paper III, Paper V), [165, 168, 169, 172-181]. Nevertheless, exposure of other cell lines to SPIO has been associated with some toxic effects such as: inflammation, the formation of apoptotic bodies, impaired mitochondrial function, membrane leakage of lactate dehydrogenase, generation of reactive oxygen species (ROS), increase in micronuclei, and chromosome condensation [182]. Therefore, more studies are needed to investigate the effects of SPIO-based contrast agents on islet cell ultrastructure and behavior.

In our next set of experiments (Paper III), we attempted to trace the fate of the iron label after transplantation as a function of islet death. Immediately after transplantation in the liver, islets retained Feridex labeling and therefore, were visible on MR images. However, as immune rejection and other factors were affecting their viability, transplanted islet cells died releasing Feridex and decreasing its content significantly. Pancreatic islet from immunocompetent mice 10 days after transplantation were infiltrated with immune cells, but were still maintaining some of the label, allowing for its detection by MRI. Interestingly, the remaining label in the islet was not internalized by invading cells, but stayed associated with islet cells. At the same time, as islets were dying, they released their content into the liver parenchyma where it was internalized and processed by Kupffer cells. By 14 days after transplantation, however, there was no evidence of iron associated with Kupffer cells or liver parenchyma, suggesting rapid clearance of the label consistent with the known pharmacokinetics of the compound [166]. From an imaging perspective, iron released by dying islet cells in small amounts diffuses throughout the liver and sparsely distributes over a larger area and therefore, is not expected to create “false positives” on MR images. In contrast, Feridex concentrated upon internalization within viable pancreatic islet cells creates a signal void due to compartmentalization of the label in a membrane-enclosed environment [183, 184]. The persistence of iron within Kuppfer cells is short-lived due to its rapid processing by these cells and its release into the physiologic iron pool [185]. On *in vivo* images upon release from dead or dying islets, the label loses its compartmentalization as it diffuses through the tissue. Using the specified gradient-echo MRI sequences, the non-compartmentalized label (diffused into interstitium) or the label localized within a single cell

(e.g. internalized by a Kupffer cell) would not generate a sufficient T2* effect in order to persist as a signal void. Only the label compartmentalized at a high concentration within a multicellular structure (i.e. pancreatic islet which consists of about 2000 cells with an average diameter of 200-400 μm) would be detectable using the specified degree of T2* weighting and spatial resolution. A single cell of a 40-fold smaller average diameter is beyond the limit of detection of MRI sequences with the particular level of T2*-weighting and spatial resolution that we are using. Therefore, the only entity within the liver, which would retain iron at a high concentration and with a steady time-course, would be viable islet grafts. Lee *et al* in their study on rats described the similar fate of the iron label [168].

In the next study, we used MRI to investigate the relationship between hyperglycemia and islet graft mass (Paper IV). Feridex-labeled islets were transplanted to healthy and diabetic immunodeficient mice. There was a visual difference in the number of islets between the groups on day 5 after transplantation presumably due to the toxic effect of hyperglycemia in diabetic animals. Furthermore, comparison of MRI data with histochemical analysis of islet grafts revealed that the disappearance of pancreatic islets on MR images was due to islet death. The half-life of the islets in diabetic mice was on average 2.6 times shorter than in healthy animals. In this study, we demonstrated that the adverse effects of hyperglycemia on transplanted pancreatic islet graft mass can be reliably monitored over an extended period of time by noninvasive MR imaging.

The next step was to evaluate the impact of islet purity on contrast agent labeling and detection of pancreatic islets by MR imaging (Paper IV). We found that iron uptake was significantly higher in high-purity islets than in low-purity islets. However, on MR images, the number of dark spots representing labeled islets appeared to be the same in both groups. The two groups of animals did not exhibit any statistically significant difference in islet disappearance rate throughout the study. In contrast, there was an increased islet cell death and macrophage infiltration in grafts contaminated with acinar and ductal tissue. These findings led us to the conclusion that there was a significant loss of contaminating tissue in mice transplanted with 50% purity islets early after the procedure. Despite the fact that this contaminating tissue appeared lightly labeled with Feridex, its fast disappearance resulted in equal islet loss rate in both models. According to our immunohistochemical assessment and morphological results obtained by other investigators, non-islet tissue mostly disappeared during the first 2 weeks after transplantation, whereas islet tissue remained well preserved [186, 187]. This study demonstrated that transplantation of islets contaminated with nonendocrine tissue did not have any significant influence on MR images, presumably because of a low labeling rate of this tissue and a fast rate of its disappearance after transplantation.

The subsequent experiment represented an essential intermediate step before translating MRI of islet transplantation from experimental to clinical applications (Paper V). We developed a comprehensive new method for visualization of transplanted islets (small structures 150 –200 μm in diameter) in a large animal model. In a preclinical non-human primate (baboon: *Papio hamadryas)* model of autologous islet transplantation, we showed that islets labeled with Feridex could be detected *in vivo* by MRI. Furthermore, we described the development of a semiautomated image analysis algorithm for the quantitative evaluation of changes in the transplanted islet mass over time. Finally, we demonstrated that the labeling technique was safe to the animal and did not adversely affect the long-term function or survival of the animal and the transplanted islets.

In diabetic patients, pancreatic islet transplantation represents an attractive alternative to whole organ transplantation. However, one of the major hurdles on the way to clinical implementation of this procedure is an inability to monitor islet noninvasively. As outlined in this thesis, significant progress has been achieved towards this goal. Validation studies in mice and in non-human primates demonstrated safety and reliability of magnetic resonance imaging for detection and monitoring of transplanted islets. In the future we envision application of this technique not only for the purpose of islet monitoring but also for image-guided therapy. To that end, the first steps have been taken to combine labeling of pancreatic islets with iron oxide nanoparticles and delivery of therapeutic load. Specifically, we attempted to deliver gene therapy to pancreatic islets prior to transplantation with the ultimate goal to silence genes responsible for islet damage. In our preliminary experiments we showed silencing of a model gene (GFP) in GFP-expressing islets following incubation with nanoparticles conjugated to siRNA to GFP [188]. We showed that siRNA conjugated to nanoparticles accumulated in isolated islets in quantities sufficient for detection by MRI *in vitro* and for silencing target model gene GFP. These investigations paved the way toward therapeutic studies where pancreatic islets were labeled with nanoparticles conjugated to siRNA targeting mRNA for caspase-3. Transplanted islets demonstrated prolonged survival compared to controls as shown by *in vivo* MRI during the initial 2-week period when islet destruction is the most prominent [189]. There are plans in the future to target other genes responsible for various aspects of islet destruction before and after islet transplantation. In addition, since iron oxide nanoparticles represent a convenient platform for conjugation chemistry, delivery of other drugs, both established and experimental, is considered as well. The ability to monitor islet survival following therapy is a significant benefit that these agents offer. This imaging modality can greatly assist clinical management of patients following pancreatic islet transplantation.

8. Final Conclusions

Magnetic resonance imaging can be used for noninvasive monitoring of pancreatic islet transplantation:

- human pancreatic islets can be labeled with the SPIO-MN-based contract agent ferumoxide (Feridex) that produces a sufficient signal-intensity change on MR images
- ferumoxide does not alter islet vitality and insulin-producing function
- ferumoxide-labeled islets can be monitored *in vivo* by MRI noninvasively and repeatedly in real time
- the relative transplanted islet mass can be quantified and tracked over time by MRI
- MRI can monitor islet death due to immune rejection or glucose toxicity noninvasively and repeatedly in real time
- islet purity does not have any impact on labeling by ferumoxide
- MRI of ferumoxide-labeled pancreatic islets can be successfully applied to a pre-clinical, non-human primate model

We anticipate that the findings obtained in these studies would ultimately result in the ability to detect and monitor pancreatic islet engraftment in humans, which would greatly aid in the clinical management of diabetic patients.

"I just think how fortunate I am. I feel fabulous. I have endless energy and a freedom I never felt before. I have so much self confidence – and no more fear."

-Islet transplant recipient Diane Gilletti

9. References

1. Daneman, D., *Type 1 diabetes.* Lancet, 2006. **367**(9513): p. 847-58.
2. N.D.F.S. *National Diabetes Fact Sheet* http://www.cdc.gov/. 2011
3. Patterson, C.C., et al., *Incidence trends for childhood type 1 diabetes in Europe during 1989-2003 and predicted new cases 2005-20: a multicentre prospective registration study.* Lancet, 2009. **373**(9680): p. 2027-33.
4. Bruno, G., et al., *The impact of diabetes on prescription drug costs: the population-based Turin study.* Diabetologia, 2008. **51**(5): p. 795-801.
5. Polychronakos, C. and Q. Li, *Understanding type 1 diabetes through genetics: advances and prospects.* Nat Rev Genet, 2011. **12**(11): p. 781-92.
6. Eugene, L., *Opie pathological changes affecting the islands of Langerhans of the pancreas.* J Boston Soc Med Sci, 1900. **4**(10): p. 251–260.
7. Todorov, I., et al., *Quantitative assessment of beta-cell apoptosis and cell composition of isolated, undisrupted human islets by laser scanning cytometry.* Transplantation, 2010. **90**(8): p. 836-42.
8. Bluestone, J.A., K. Herold, and G. Eisenbarth, *Genetics, pathogenesis and clinical interventions in type 1 diabetes.* Nature, 2010. **464**(7293): p. 1293-300.
9. Willcox, A., et al., *Analysis of islet inflammation in human type 1 diabetes.* Clin Exp Immunol, 2009. **155**(2): p. 173-81.
10. Association, A.D., *Standards of medical care in diabetes--2010.* Diabetes Care, 2010 **33**(Suppl 1): p. S11-61.
11. DCCT, *The Diabetes Control and Complications Trial Research Group. The effect of intensive treatment of diabetes on the development and progression of long-term complications in insulin-dependent diabetes mellitus.* N. Engl. J. Med., 1993. **329** (14): p. 977–986.
12. DCCT, *The Diabetes Control and Complications Trial Research Group. Hypoglycemia in the Diabetes Control and Complications Trial. The Diabetes Control and Complications Trial Research Group.* Diabetes, 1997. **46**(2): p. 271–286.
13. DCCT, *The Diabetes Control and Complications Trial/Epidemiology of Diabetes Interventions and Complications Study Research Group. Intensive diabetes treatment and cardiovascular disease in patients with type 1 diabetes.* N Engl J Med 2005. **353**: p. 2643–2653.
14. Cryer, P.E., *The barrier of hypoglycemia in diabetes.* Diabetes, 2008. **57**(12): p. 3169-76.
15. Paris, C.A., et al., *Predictors of insulin regimens and impact on outcomes in youth with type 1 diabetes: the SEARCH for Diabetes in Youth study.* J Pediatr, 2009. **155**(2): p. 183-9 e1.
16. Mortensen, H.B. and P. Hougaard, *Comparison of metabolic control in a cross-sectional study of 2,873 children and adolescents with IDDM from 18 countries. The Hvidore Study Group on Childhood Diabetes.* Diabetes Care, 1997. **20**(5): p. 714-20.
17. Tamborlane, W.V., et al., *Continuous glucose monitoring and intensive treatment of type 1 diabetes.* N Engl J Med, 2008. **359**(14): p. 1464-76.
18. Cheung, B.M., et al., *Diabetes prevalence and therapeutic target achievement in the United States, 1999 to 2006.* Am J Med, 2009. **122**(5): p. 443-53.

19. Kumareswaran, K., M.L. Evans, and R. Hovorka, *Closed-loop insulin delivery: towards improved diabetes care.* Discov Med, 2012. **13**(69): p. 159-70.
20. Ryan, E.A., *Pancreas transplants: for whom?* Lancet, 1998. **351**(9109): p. 1072-3.
21. Dixon, S., et al., *The role of interventional radiology and imaging in pancreatic islet cell transplantation.* Clin Radiol, 2012.
22. Froud, T., et al., *Islet transplantation in type 1 diabetes mellitus using cultured islets and steroid-free immunosuppression: Miami experience.* Am J Transplant, 2005. **5**(8): p. 2037-46.
23. Ricordi, C., *Islet transplantation: a brave new world.* Diabetes, 2003. **52**(7): p. 1595-603.
24. Shapiro, A., et al., *Islet transplantation in seven patients with type 1 diabetes mellitus using a glucocorticoid-free immunosuppressive regimen.* N Engl J Med, 2000. **343**: p. 230-238.
25. Ricordi, C., B.J. Hering, and A.M. Shapiro, *Beta-cell transplantation for diabetes therapy.* Lancet, 2008. **372**(9632): p. 27-8; author reply 29-30.
26. Low, G., et al., *Role of imaging in clinical islet transplantation.* Radiographics, 2010. **30**(2): p. 353-66.
27. Ballinger, W.F. and P.E. Lacy, *Transplantation of intact pancreatic islets in rats.* Surgery, 1972. **72**(2): p. 175-86.
28. Kemp, C.B., et al., *Transplantation of isolated pancreatic islets into the portal vein of diabetic rats.* Nature, 1973. **244**(5416): p. 447.
29. Najarian, J.S., et al., *Total or near total pancreatectomy and islet autotransplantation for treatment of chronic pancreatitis.* Ann Surg, 1980. **192**(4): p. 526-42.
30. Largiader, F., et al., *[Successful allotransplantation of an island of Langerhans].* Schweiz Med Wochenschr, 1979. **109**(45): p. 1733-6.
31. M, B., *International Islet Transplant Registry Newsletter No. 9.* 2001. **8**(1).
32. Lakey, J.R., M. Mirbolooki, and A.M. Shapiro, *Current status of clinical islet cell transplantation.* Methods Mol Biol, 2006. **333**: p. 47-104.
33. Feutren, G. and M.J. Mihatsch, *Risk factors for cyclosporine-induced nephropathy in patients with autoimmune diseases. International Kidney Biopsy Registry of Cyclosporine in Autoimmune Diseases.* N Engl J Med, 1992. **326**(25): p. 1654-60.
34. Ryan, E., et al., *Clinical outcomes and insulin secretion after islet transplantation with the Edmonton protocol.* Diabetes, 2001. **50**: p. 710-719.
35. Ryan, E., et al., *Successful islet transplantation: continued insulin reserve provides long-term glycemic control.* Diabetes, 2002. **51**: p. 2148-2157.
36. Shapiro, A., C. Ricordi, and B. Hering, *Edmonton's islet success has indeed been replicated elsewhere.* Lancet, 2003. **362**: p. 1242.
37. Shapiro, A.M., et al., *International trial of the Edmonton protocol for islet transplantation.* N Engl J Med, 2006. **355**(13): p. 1318-30.
38. Hering, B.J., et al., *Single-donor, marginal-dose islet transplantation in patients with type 1 diabetes.* Jama, 2005. **293**(7): p. 830-5.
39. CITR, *Collaborative Islet Transplant Registry annual report* 2010.
40. Frank, A., et al., *Transplantation for type I diabetes: comparison of vascularized whole-organ pancreas with isolated pancreatic islets.* Ann Surg, 2004. **240**(4): p. 631-40; discussion 640-3.
41. Markmann, J.F., et al., *Insulin independence following isolated islet transplantation and single islet infusions.* Ann Surg, 2003. **237**(6): p. 741-9; discussion 749-50.

42. Casey, J.J., et al., *Portal venous pressure changes after sequential clinical islet transplantation.* Transplantation, 2002. **74**(7): p. 913-5.
43. Lakey, J.R., P.W. Burridge, and A.M. Shapiro, *Technical aspects of islet preparation and transplantation.* Transpl Int, 2003. **16**(9): p. 613-32.
44. Paraskevas, S., et al., *Cell loss in isolated human islets occurs by apoptosis.* Pancreas, 2000. **20**(3): p. 270-6.
45. Brandhorst, D., et al., *Influence of donor data and organ procurement on human islet isolation.* Transplant Proc, 1994. **26**(2): p. 592-3.
46. Kuhtreiber, W.M., et al., *Islet isolation from human pancreas with extended cold ischemia time.* Transplant Proc, 2010. **42**(6): p. 2027-31.
47. Ricordi, C., et al., *Automated method for isolation of human pancreatic islets.* Diabetes, 1988. **37**(4): p. 413-20.
48. Nano, R., et al., *Islet isolation for allotransplantation: variables associated with successful islet yield and graft function.* Diabetologia, 2005. **48**(5): p. 906-12.
49. Deters, N.A., R.A. Stokes, and J.E. Gunton, *Islet transplantation: factors in short-term islet survival.* Arch Immunol Ther Exp (Warsz), 2011. **59**(6): p. 421-9.
50. Bottino, R., et al., *Response of human islets to isolation stress and the effect of antioxidant treatment.* Diabetes, 2004. **53**(10): p. 2559-68.
51. Bottino, R., et al., *Preservation of human islet cell functional mass by anti-oxidative action of a novel SOD mimic compound.* Diabetes, 2002. **51**(8): p. 2561-7.
52. Azevedo-Martins, A.K., et al., *Improvement of the mitochondrial antioxidant defense status prevents cytokine-induced nuclear factor-kappaB activation in insulin-producing cells.* Diabetes, 2003. **52**(1): p. 93-101.
53. Kajikawa, M., et al., *Ouabain suppresses glucose-induced mitochondrial ATP production and insulin release by generating reactive oxygen species in pancreatic islets.* Diabetes, 2002. **51**(8): p. 2522-9.
54. Piganelli, J.D., et al., *A metalloporphyrin-based superoxide dismutase mimic inhibits adoptive transfer of autoimmune diabetes by a diabetogenic T-cell clone.* Diabetes, 2002. **51**(2): p. 347-55.
55. Stendahl, J.C., D.B. Kaufman, and S.I. Stupp, *Extracellular matrix in pancreatic islets: relevance to scaffold design and transplantation.* Cell Transplant, 2009. **18**(1): p. 1-12.
56. Thomas, F.T., et al., *Anoikis, extracellular matrix, and apoptosis factors in isolated cell transplantation.* Surgery, 1999. **126**(2): p. 299-304.
57. Frisch, S.M. and E. Ruoslahti, *Integrins and anoikis.* Curr Opin Cell Biol, 1997. **9**(5): p. 701-6.
58. Russ, H.A., et al., *In vitro proliferation of cells derived from adult human beta-cells revealed by cell-lineage tracing.* Diabetes, 2008. **57**(6): p. 1575-83.
59. Weinberg, N., et al., *Lineage tracing evidence for in vitro dedifferentiation but rare proliferation of mouse pancreatic beta-cells.* Diabetes, 2007. **56**(5): p. 1299-304.
60. Negi, S., et al., *Analysis of beta-cell gene expression reveals inflammatory signaling and evidence of dedifferentiation following human islet isolation and culture.* PLoS One, 2012. **7**(1): p. e30415.
61. McDonald, E., et al., *The emerging role of SOX transcription factors in pancreatic endocrine cell development and function.* Stem Cells Dev, 2009. **18**(10): p. 1379-88.
62. Davalli, A., et al., *A selective decrease in the beta cell mass of human islets transplanted into diabetic nude mice.* Transplantation, 1995. **59**: p. 817-820.

63. Davalli, A., et al., *Vulnerability of islets in the immediate posttransplantation period. Dynamic changes in structure and function.* Diabetes, 1996. **45**: p. 1161-1167.
64. Biarnes, M., et al., *Beta-cell death and mass in syngeneically transplanted islets exposed to short- and long-term hyperglycemia.* Diabetes, 2002. **51**(1): p. 66-72.
65. Barshes, N., S. Wyllie, and J. Goss, *Inflammation-mediated dysfunction and apoptosis in pancreatic islet transplantation: implications for intrahepatic grafts.* J Leukocyte Biol, 2005. **77**: p. 587-597.
66. Lai, Y., C. Chen, and T. Linn, *Innate immunity and heat shock response in islet transplantation.* Clin Exp Immunol, 2009. **157**(1): p. 1-8.
67. Gysemans, C., et al., *Cytokine signalling in the beta-cell: a dual role for IFNgamma.* Biochem Soc Trans, 2008. **36**(Pt 3): p. 328-33.
68. Biozzi, G., B. Benacerraf, and B.N. Halpern, *Quantitative study of the granulopectic activity of the reticulo-endothelial system. II. A study of the kinetics of the R. E. S. in relation to the dose of carbon injected; relationship between the weight of the organs and their activity.* Br J Exp Pathol, 1953. **34**(4): p. 441-57.
69. Bottino, R., et al., *Transplantation of allogeneic islets of Langerhans in the rat liver: effects of macrophage depletion on graft survival and microenvironment activation.* Diabetes, 1998. **47**: p. 316-323.
70. Piemonti, L., et al., *Human pancreatic islets produce and secrete MCP-1/CCL2: relevance in human islet transplantation.* Diabetes, 2002. **51**(1): p. 55-65.
71. Ehrnfelt, C., et al., *Adult porcine islets produce MCP-1 and recruit human monocytes in vitro.* Xenotransplantation, 2004. **11**(2): p. 184-94.
72. Omer, A., et al., *Macrophage depletion improves survival of porcine neonatal pancreatic cell clusters contained in alginate macrocapsules transplanted into rats.* Xenotransplantation, 2003. **10**(3): p. 240-51.
73. Colletti, L.M., et al., *Role of tumor necrosis factor-alpha in the pathophysiologic alterations after hepatic ischemia/reperfusion injury in the rat.* J Clin Invest, 1990. **85**(6): p. 1936-43.
74. Caldwell-Kenkel, J.C., et al., *Kupffer cell activation and endothelial cell damage after storage of rat livers: effects of reperfusion.* Hepatology, 1991. **13**(1): p. 83-95.
75. Gray, D.W., et al., *Exocrine contamination impairs implantation of pancreatic islets transplanted beneath the kidney capsule.* J Surg Res, 1988. **45**(5): p. 432-42.
76. Johansson, H., et al., *Tissue factor produced by the endocrine cells of the islets of Langerhans is associated with a negative outcome of clinical islet transplantation.* Diabetes, 2005. **54**(6): p. 1755-62.
77. Moberg, L., et al., *Production of tissue factor by pancreatic islet cells as a trigger of detrimental thrombotic reactions in clinical islet transplantation.* Lancet, 2002. **360**(9350): p. 2039-45.
78. Moberg, L., O. Korsgren, and B. Nilsson, *Neutrophilic granulocytes are the predominant cell type infiltrating pancreatic islets in contact with ABO-compatible blood.* Clin Exp Immunol, 2005. **142**(1): p. 125-31.
79. Moberg, L., *The role of the innate immunity in islet transplantation.* Ups J Med Sci, 2005. **110**(1): p. 17-55.
80. Ozmen, L., et al., *Inhibition of thrombin abrogates the instant blood-mediated inflammatory reaction triggered by isolated human islets: possible application of the*

thrombin inhibitor melagatran in clinical islet transplantation. Diabetes, 2002. **51**(6): p. 1779-84.
81. Bennet, W., et al., *Isolated human islets trigger an instant blood mediated inflammatory reaction: implications for intraportal islet transplantation as a treatment for patients with type 1 diabetes.* Ups J Med Sci, 2000. **105**(2): p. 125-33.
82. Tjernberg, J., et al., *Acute antibody-mediated complement activation mediates lysis of pancreatic islets cells and may cause tissue loss in clinical islet transplantation.* Transplantation, 2008. **85**(8): p. 1193-9.
83. Dionne, K.E., C.K. Colton, and M.L. Yarmush, *Effect of hypoxia on insulin secretion by isolated rat and canine islets of Langerhans.* Diabetes, 1993. **42**(1): p. 12-21.
84. Cabrera, O., et al., *The unique cytoarchitecture of human pancreatic islets has implications for islet cell function.* Proc Natl Acad Sci U S A, 2006. **103**(7): p. 2334-9.
85. Kim, A., et al., *Computer-assisted large-scale visualization and quantification of pancreatic islet mass, size distribution and architecture.* J Vis Exp, 2011(49).
86. Griffith, R.C., et al., *A morphologic study of intrahepatic portal-vein islet isografts.* Diabetes, 1977. **26**(3): p. 201-14.
87. Jansson, L. and P.O. Carlsson, *Graft vascular function after transplantation of pancreatic islets.* Diabetologia, 2002. **45**(6): p. 749-63.
88. Menger, M.D., et al., *Angiogenesis and hemodynamics of microvasculature of transplanted islets of Langerhans.* Diabetes, 1989. **38 Suppl 1**: p. 199-201.
89. Nyqvist, D., et al., *Donor islet endothelial cells participate in formation of functional vessels within pancreatic islet grafts.* Diabetes, 2005. **54**(8): p. 2287-93.
90. Brissova, M. and A.C. Powers, *Revascularization of transplanted islets: can it be improved?* Diabetes, 2008. **57**(9): p. 2269-71.
91. Vasir, B., et al., *Gene expression of VEGF and its receptors Flk-1/KDR and Flt-1 in cultured and transplanted rat islets.* Transplantation, 2001. **71**(7): p. 924-35.
92. Vajkoczy, P., et al., *Angiogenesis and vascularization of murine pancreatic islet isografts.* Transplantation, 1995. **60**(2): p. 123-7.
93. Korsgren, O., et al., *Optimising islet engraftment is critical for successful clinical islet transplantation.* Diabetologia, 2008. **51**(2): p. 227-32.
94. Parks, D.A. and D.N. Granger, *Contributions of ischemia and reperfusion to mucosal lesion formation.* Am J Physiol, 1986. **250**(6 Pt 1): p. G749-53.
95. Korthuis, R.J., J.K. Smith, and D.L. Carden, *Hypoxic reperfusion attenuates postischemic microvascular injury.* Am J Physiol, 1989. **256**(1 Pt 2): p. H315-9.
96. Carlsson, P.O., et al., *Markedly decreased oxygen tension in transplanted rat pancreatic islets irrespective of the implantation site.* Diabetes, 2001. **50**(3): p. 489-95.
97. Wang, X., et al., *B7-H4 Pathway in Islet Transplantation and beta-Cell Replacement Therapies.* J Transplant, 2011. **2011**: p. 418902.
98. Bellin, M.D., et al., *Potent induction immunotherapy promotes long-term insulin independence after islet transplantation in type 1 diabetes.* Am J Transplant, 2012. **12**(6): p. 1576-83.
99. Wood, K.J. and R. Goto, *Mechanisms of rejection: current perspectives.* Transplantation, 2012. **93**(1): p. 1-10.
100. Mineo, D., et al., *Minimization and withdrawal of steroids in pancreas and islet transplantation.* Transpl Int, 2009. **22**(1): p. 20-37.

101. Johnson, J.D., et al., *Different effects of FK506, rapamycin, and mycophenolate mofetil on glucose-stimulated insulin release and apoptosis in human islets.* Cell Transplant, 2009. **18**(8): p. 833-45.
102. Zhang, N., et al., *Sirolimus is associated with reduced islet engraftment and impaired beta-cell function.* Diabetes, 2006. **55**(9): p. 2429-36.
103. Balamurugan, A.N., et al., *Prospective and challenges of islet transplantation for the therapy of autoimmune diabetes.* Pancreas, 2006. **32**(3): p. 231-43.
104. Braghi, S., et al., *Modulation of humoral islet autoimmunity by pancreas allotransplantation influences allograft outcome in patients with type 1 diabetes.* Diabetes, 2000. **49**(2): p. 218-24.
105. Kaneto, H., et al., *Beneficial effects of antioxidants in diabetes: possible protection of pancreatic beta-cells against glucose toxicity.* Diabetes, 1999. **48**(12): p. 2398-406.
106. Eizirik, D.L., G.S. Korbutt, and C. Hellerstrom, *Prolonged exposure of human pancreatic islets to high glucose concentrations in vitro impairs the beta-cell function.* J Clin Invest, 1992. **90**(4): p. 1263-8.
107. Weir, G.C. and S. Bonner-Weir, *Five stages of evolving beta-cell dysfunction during progression to diabetes.* Diabetes, 2004. **53 Suppl 3**: p. S16-21.
108. Leibowitz, G., et al., *beta]-cell glucotoxicity in the psammomys obesus model of type 2 diabetes.* Diabetes, 2001. **50**: p. S113-S117.
109. Maedler, K., et al., *Glucose-induced beta cell production of IL-1beta contributes to glucotoxicity in human pancreatic islets.* J Clin Invest, 2002. **110**(6): p. 851-60.
110. Laybutt, D.R., et al., *Influence of diabetes on the loss of beta cell differentiation after islet transplantation in rats.* Diabetologia, 2007. **50**(10): p. 2117-25.
111. Robertson, R.P. and J.S. Harmon, *Diabetes, glucose toxicity, and oxidative stress: A case of double jeopardy for the pancreatic islet beta cell.* Free Radic Biol Med, 2006. **41**(2): p. 177-84.
112. Makhlouf, L., et al., *Importance of hyperglycemia on the primary function of allogeneic islet transplants.* Transplantation, 2003. **76**(4): p. 657-64.
113. Melzi, R., et al., *Relevance of hyperglycemia on the timing of functional loss of allogeneic islet transplants: implication for mouse model.* Transplantation, 2007. **83**(2): p. 167-73.
114. Montana, E., S. Bonner-Weir, and G. Weir, *Beta-cell mass and growth after syngeneic islet cell transplantation in normal and streptozotocin diabetic C57BL/6 mice.* J Clin Invest, 1993. **91**: p. 780-787.
115. Jansson, L., et al., *Impairment of glucose-induced insulin secretion in human pancreatic islets transplanted to diabetic nude mice.* J Clin Invest, 1995. **96**(2): p. 721-6.
116. Eizirik, D.L., et al., *Mechanisms of defective glucose-induced insulin release in human pancreatic islets transplanted to diabetic nude mice.* J Clin Endocrinol Metab, 1997. **82**(8): p. 2660-3.
117. Nacher, V., et al., *Normoglycemia restores beta-cell replicative response to glucose in transplanted islets exposed to chronic hyperglycemia.* Diabetes, 1998. **47**(2): p. 192-6.
118. Devaraj, S., et al., *Hyperglycemia induces monocytic release of interleukin-6 via induction of protein kinase c-{alpha} and -{beta}.* Diabetes, 2005. **54**(1): p. 85-91.
119. Wautier, J.L., E. Boulanger, and M.P. Wautier, *Postprandial hyperglycemia alters inflammatory and hemostatic parameters.* Diabetes Metab, 2006. **32 Spec No2**: p. 2S34-6.

120. Thompson, D.M., et al., *Reduced progression of diabetic microvascular complications with islet cell transplantation compared with intensive medical therapy.* Transplantation, 2011. **91**(3): p. 373-8.
121. Berney, T. and C. Toso, *Monitoring of the islet graft.* Diabetes Metab, 2006. **32**(5 Pt 2): p. 503-12.
122. Pileggi, A., et al., *Overcoming the challenges now limiting islet transplantation: a sequential, integrated approach.* Ann N Y Acad Sci, 2006. **1079**: p. 383-98.
123. Bhargava, R., et al., *Prevalence of hepatic steatosis after islet transplantation and its relation to graft function.* Diabetes, 2004. **53**(5): p. 1311-7.
124. Eckhard, M., et al., *Disseminated periportal fatty degeneration after allogeneic intraportal islet transplantation in a patient with type 1 diabetes mellitus: a case report.* Transplant Proc, 2004. **36**(4): p. 1111-6.
125. Sakata, N., et al., *MRI assessment of ischemic liver after intraportal islet transplantation.* Transplantation, 2009. **87**(6): p. 825-30.
126. Markmann, J.F., et al., *Magnetic resonance-defined periportal steatosis following intraportal islet transplantation: a functional footprint of islet graft survival?* Diabetes, 2003. **52**(7): p. 1591-4.
127. Westermark, G.T., et al., *Widespread amyloid deposition in transplanted human pancreatic islets.* N Engl J Med, 2008. **359**(9): p. 977-9.
128. Weissleder, R. and U. Mahmood, *Molecular imaging.* Radiology, 2001. **219**(2): p. 316-33.
129. Massoud, T. and S. Gambhir, *Molecular imaging in living subjects: seeing fundamental biological processes in a new light.* Genes & Development, 2003. **17**: p. 545-580.
130. Wang, P., Z. Medarova, and A. Moore, *Molecular imaging: a promising tool to monitor islet transplantation.* J Transplant, 2011. **2011**: p. 202915.
131. Borot, S., et al., *Noninvasive imaging techniques in islet transplantation.* Curr Diab Rep, 2011. **11**(5): p. 375-83.
132. Kaufman D, B.M., Nelson J, Zhang X, Chen X., *In vivo, real-time, non-invasive bioluminescent imaging of transplanted islets in a functional murine model.* In:Imaging the Pancreatic Beta Cell. Bethesda, MD, 2003.
133. Powers A, F.M., Virostko J, et al., *Using bioluminescence to non-invasively image and assess transplanted islet mass.* In:Imaging the Pancreatic Beta Cell. Bethesda, MD, 2003.
134. Lu, Y., et al., *Bioluminescent monitoring of islet graft survival after transplantation.* Mol Ther, 2004. **9**(3): p. 428-35.
135. Virostko, J., et al., *Factors influencing quantification of in vivo bioluminescence imaging: application to assessment of pancreatic islet transplants.* Mol Imaging, 2004. **3**(4): p. 333-42.
136. Fowler, M., et al., *Assessment of pancreatic islet mass after islet transplantation using in vivo bioluminescence imaging.* Transplantation, 2005. **79**(7): p. 768-76.
137. Park, S.Y., et al., *Optical imaging of pancreatic beta cells in living mice expressing a mouse insulin I promoter-firefly luciferase transgene.* Genesis, 2005. **43**(2): p. 80-6.
138. Chen, X., et al., *In vivo bioluminescence imaging of transplanted islets and early detection of graft rejection.* Transplantation, 2006. **81**(10): p. 1421-7.
139. Virostko, J., et al., *Bioluminescence imaging in mouse models quantifies beta cell mass in the pancreas and after islet transplantation.* Mol Imaging Biol, 2010. **12**(1): p. 42-53.

140. Medarova, Z. and A. Moore, *Non-invasive detection of transplanted pancreatic islets.* Diabetes Obes Metab, 2008. **10 Suppl 4**: p. 88-97.
141. Bertera, S., et al., *Body window-enabled in vivo multicolor imaging of transplanted mouse islets expressing an insulin-Timer fusion protein.* BioTechniques, 2003. **35**(4): p. 718-22.
142. Fan, Z., et al., *In vivo tracking of 'color-coded' effector, natural and induced regulatory T cells in the allograft response.* Nat Med, 2010. **16**(6): p. 718-22.
143. Phelps, M.E., *Positron emission tomography provides molecular imaging of biological processes.* Proc Natl Acad Sci U S A, 2000. **97**(16): p. 9226-33.
144. Eich, T., et al., *Positron emission tomography: a real-time tool to quantify early islet engraftment in a preclinical large animal model.* Transplantation, 2007. **84**(7): p. 893-8.
145. Eich, T., O. Eriksson, and T. Lundgren, *Visualization of early engraftment in clinical islet transplantation by positron-emission tomography.* N Engl J Med, 2007. **356**(26): p. 2754-5.
146. Eriksson, O., et al., *Positron emission tomography in clinical islet transplantation.* Am J Transplant, 2009. **9**(12): p. 2816-24.
147. Sokoloff, L., et al., *The [14C]deoxyglucose method for the measurement of local cerebral glucose utilization: theory, procedure, and normal values in the conscious and anesthetized albino rat.* J Neurochem, 1977. **28**(5): p. 897-916.
148. Kim, S.J., et al., *Quantitative micro positron emission tomography (PET) imaging for the in vivo determination of pancreatic islet graft survival.* Nat Med, 2006. **12**(12): p. 1423-8.
149. Lu, Y., et al., *Noninvasive imaging of islet grafts using positron-emission tomography.* Proc Natl Acad Sci U S A, 2006. **103**(30): p. 11294-9.
150. Lu, Y., et al., *Long-term monitoring of transplanted islets using positron emission tomography.* Mol Ther, 2006. **14**(6): p. 851-6.
151. Kim, S.J., et al., *Inhibition of dipeptidyl peptidase IV with sitagliptin (MK0431) prolongs islet graft survival in streptozotocin-induced diabetic mice.* Diabetes, 2008. **57**(5): p. 1331-9.
152. Eriksson, O. and A. Alavi, *Imaging the islet graft by positron emission tomography.* Eur J Nucl Med Mol Imaging, 2012. **39**(3): p. 533-42.
153. Wu, Z., et al., *In vivo imaging of transplanted islets with 64Cu-DO3A-VS-Cys40-Exendin-4 by targeting GLP-1 receptor.* Bioconjug Chem, 2011. **22**(8): p. 1587-94.
154. Modo, M., M. Hoehn, and J.W. Bulte, *Cellular MR imaging.* Mol Imaging, 2005. **4**(3): p. 143-64.
155. Bulte, J.W., *In vivo MRI cell tracking: clinical studies.* AJR Am J Roentgenol, 2009. **193**(2): p. 314-25.
156. Shen, T., et al., *Monocrystalline iron oxide nanocompounds (MION): physicochemical properties.* Magn Reson Med, 1993. **29**(5): p. 599-604.
157. Weissleder, R., *Scaling down imaging: molecular mapping of cancer in mice.* Nat Review, 2002. **2**(1): p. 11-18.
158. Moore, A., et al., *MR Imaging of insulitis in autoimmune diabetes.* Magn Reson Med, 2002. **47**: p. 751-758.
159. Moore, A., et al., *In vivo targeting of underglycosylated MUC-1 tumor antigen using a multi-modal imaging probe.* Cancer Res, 2004. **64**: p. 1821-1827.
160. Moore, A., S. Bonner-Weir, and R. Weissleder, *Non-invasive in vivo measurement of beta-cell mass in mouse model of diabetes.* Diabetes, 2001. **50**: p. 2231-2236.

161. Medarova, Z., et al., *Imaging b-cell death with a near-infrared probe.* Diabetes, 2004. **54**: p. 1780-1788.
162. Massoud, T.F. and S.S. Gambhir, *Molecular imaging in living subjects: seeing fundamental biological processes in a new light.* Genes Dev, 2003. **17**(5): p. 545-80.
163. Medarova, Z. and A. Moore, *MRI in diabetes: first results.* AJR Am J Roentgenol, 2009. **193**(2): p. 295-303.
164. Mills, P.H. and E.T. Ahrens, *Theoretical MRI contrast model for exogenous T2 agents.* Magn Reson Med, 2007. **57**(2): p. 442-7.
165. Jirak, D., et al., *MRI of transplanted pancreatic islets.* Magn Res Med, 2004. **52**: p. 1228-1233.
166. Sosnovik, D.E., M. Nahrendorf, and R. Weissleder, *Magnetic nanoparticles for MR imaging: agents, techniques and cardiovascular applications.* Basic Res Cardiol, 2008. **103**(2): p. 122-30.
167. Kriz, J., et al., *Magnetic resonance imaging of pancreatic islets in tolerance and rejection.* Transplantation, 2005. **80**(11): p. 1596-603.
168. Lee, N., et al., *Magnetosome-like ferrimagnetic iron oxide nanocubes for highly sensitive MRI of single cells and transplanted pancreatic islets.* Proc Natl Acad Sci U S A, 2011. **108**(7): p. 2662-7.
169. Jiao, Y., et al., *Assessment of islet graft survival using a 3.0-Tesla magnetic resonance scanner.* Anat Rec (Hoboken), 2008. **291**(12): p. 1684-92.
170. Berkova, Z., et al., *Labeling of pancreatic islets with iron oxide nanoparticles for in vivo detection with magnetic resonance.* Transplantation, 2008. **85**(1): p. 155-9.
171. Arbab, A.S., et al., *A model of lysosomal metabolism of dextran coated superparamagnetic iron oxide (SPIO) nanoparticles: implications for cellular magnetic resonance imaging.* NMR Biomed, 2005. **18**(6): p. 383-9.
172. Malosio, M.L., et al., *Improving the procedure for detection of intrahepatic transplanted islets by magnetic resonance imaging.* Am J Transplant, 2009. **9**(10): p. 2372-82.
173. Ris, F., et al., *Assessment of human islet labeling with clinical grade iron nanoparticles prior to transplantation for graft monitoring by MRI.* Cell Transplant, 2010. **19**(12): p. 1573-85.
174. Zhang, S., et al., *Tracking intrahepatically transplanted islets labeled with Feridex-polyethyleneimine complex using a clinical 3.0-T magnetic resonance imaging scanner.* Pancreas, 2009. **38**(3): p. 293-302.
175. Kim, H.S., et al., *Magnetic resonance imaging and biological properties of pancreatic islets labeled with iron oxide nanoparticles.* NMR Biomed, 2009. **22**(8): p. 852-6.
176. Kim, H.S., et al., *Evaluation of porcine pancreatic islets transplanted in the kidney capsules of diabetic mice using a clinically approved superparamagnetic iron oxide (SPIO) and a 1.5T MR scanner.* Korean J Radiol, 2010. **11**(6): p. 673-82.
177. Park, K.S., et al., *Improved quantification of islet transplants by magnetic resonance imaging with Resovist.* Pancreas, 2011. **40**(6): p. 911-9.
178. Toso, C., et al., *Clinical magnetic resonance imaging of pancreatic islet grafts after iron nanoparticle labeling.* Am J Transplant, 2008. **8**(3): p. 701-6.
179. Huang, H., et al., *Labeling transplanted mice islet with polyvinylpyrrolidone coated superparamagnetic iron oxide nanoparticles for in vivo detection by magnetic resonance imaging.* Nanotechnology, 2009. **20**(36): p. 365101.

180. Juang, J.H., et al., *Magnetic resonance imaging of transplanted mouse islets labeled with chitosan-coated superparamagnetic iron oxide nanoparticles.* Transplant Proc, 2010. **42**(6): p. 2104-8.
181. Tai, J.H., et al., *Imaging islets labeled with magnetic nanoparticles at 1.5 Tesla.* Diabetes, 2006. **55**(11): p. 2931-8.
182. Singh, N., et al., *Potential toxicity of superparamagnetic iron oxide nanoparticles (SPION).* Nano Rev, 2010. **1**.
183. Moore, A., et al., *Tumoral distribution of long-circulating dextran-coated iron oxide nanoparticles in a rodent model.* Radiology, 2000. **214**: p. 568-574.
184. Bodganov, A., et al., *Trapping of dextran-coated colloids in liposomes by transient binding to aminophospholipid: preparation of ferrosomes.* Biochim Biophys Acta, 1994. **1193**: p. 212-218.
185. Weissleder, R., et al., *Superparamagnetic iron oxide: pharmacokinetics and toxicity.* Am J Roentgenol, 1989. **152**: p. 167-173.
186. Grotting, J.C., et al., *The fate of intraportally transplanted islets in diabetic rats. A morphologic and immunohistochemical study.* Am J Pathol, 1978. **92**(3): p. 653-70.
187. Franklin, W.A., J.A. Schulak, and C.R. Reckard, *The fate of transplanted pancreatic islets in the rat.* Am J Pathol, 1979. **94**(1): p. 85-95.
188. Medarova, Z., et al., *Multifunctional magnetic nanocarriers for image-tagged SiRNA delivery to intact pancreatic islets.* Transplantation, 2008. **86**(9): p. 1170-7.
189. Wang, P., et al., *Combined small interfering RNA therapy and in vivo magnetic resonance imaging in islet transplantation.* Diabetes, 2011. **60**(2): p. 565-71.

Paper I

Paper II

Paper III

Paper IV

Paper V

ISBN xxx-xx-xxxx-xxx-x